

Cite this: *Dalton Trans.*, 2025, **54**, 16285

# Biochemical assays for evaluating anticancer activity and validating mechanisms of action in coordination/organometallic compounds: a review

Dalal Alezi,<sup>a</sup> Abrar S. Iskandrani,<sup>a</sup> Ehab M. M. Ali<sup>b,c</sup> and Bandar A. Babgi<sup>\*a</sup>

Research on metal-based coordination and organometallic compounds is flourishing due to their potential to overcome drug resistance, reduce systemic toxicity, and target diverse cellular pathways. Driven by the success of cisplatin and other Pt-based drugs, transition metal complexes such as Pt(II/IV), Ru(II/III), Au(I/III), Cu(I/II), and Pd(II) have been widely investigated for their ability to interact with biomolecular targets, including DNA, proteins, and enzymes. However, the development of effective anticancer metallodrugs requires rigorous mechanistic validation, as this field is often hindered by overinterpretation and poorly designed studies. This review emphasizes the necessity of multi-assay strategies, integrating classical cytotoxicity and apoptosis assays with advanced methods such as CETSA and TPP, to clarify mechanisms of action. By correlating assay outcomes with molecular mechanisms, including redox modulation, apoptosis, proteasome inhibition, and non-apoptotic pathways such as ferroptosis and necroptosis, researchers can design more selective and multitargeted agents. This approach aims to enhance reproducibility, prevent overinterpretation, and accelerate mechanism-based drug development.

Received 2nd August 2025,  
Accepted 17th September 2025

DOI: 10.1039/d5dt01851j

rsc.li/dalton

## 1 Introduction

Despite the huge advancements in diagnosis, surgical techniques, and radiotherapy, cancer remains one of the health challenges in the 21<sup>st</sup> century, accounting for millions of deaths annually. The WHO estimated 9.7 million deaths would occur due to cancer in 2022.<sup>1</sup> Chemotherapy is a major cancer treatment, particularly for aggressive and metastatic types. However, the acquired drug resistance, systemic toxicity, severe side effects and limited selectivity of many chemotherapeutic agents necessitate the continuous exploration of alternative therapeutic agents. In this context, metal-based coordination compounds have emerged as a promising class of chemotherapeutics, offering novel modes of action distinct from organic small-molecule drugs.

Among the most extensively studied classes are coordination and organometallic complexes incorporating transition metals such as platinum (Pt),<sup>2,3</sup> ruthenium (Ru),<sup>4,5</sup> gold (Au),<sup>6,7</sup> copper (Cu),<sup>8,9</sup> and palladium (Pd).<sup>10</sup> These com-

pounds demonstrate promising anticancer activity attributed to their tunable physicochemical properties, including variable oxidation states, flexible coordination geometries, and controlled ligand exchange kinetics. Indeed, several Pt-based drugs have been approved for chemotherapy world-wide, including cisplatin, carboplatin, and oxaliplatin, while others like nedaplatin, lobaplatin, and heptaplatin have gained approvals regionally.<sup>11</sup> The capacity of metal-based complexes to interact with key biomolecular targets such as DNA, proteins, and enzymes makes them potentially therapeutically active.<sup>11,12</sup> Moreover, their redox activity enables them to generate reactive oxygen species (ROS) which induce cytotoxic stress with potential selectivity in cancer cells (cancerous cells have altered redox homeostasis compared with normal cells).<sup>11,12</sup>

To evaluate the mechanisms by which these compounds exert their anticancer effects, a range of *in vitro* biochemical assays have been developed. These assays provide critical findings, facilitating the exploration of the mechanism of action and establishing both structure–activity relationships and drug development strategies. So far, metal-based compounds function through major mechanistic pathways including:<sup>11,12</sup>

- DNA binding and damage: many metal-based drugs interact with DNA through intercalation, groove binding, or covalent binding, leading to replication stress that causes cell death.

<sup>a</sup>Department of Chemistry, Faculty of Science, King Abdulaziz University, P.O. Box 80203, Jeddah 21589, Saudi Arabia. E-mail: bbabgi@kau.edu.sa;  
Tel: +966 555563702

<sup>b</sup>Department of Biochemistry, Faculty of Science, King Abdulaziz University, P.O. Box 80203, Jeddah 21589, Saudi Arabia

<sup>c</sup>Division of Biochemistry, Department of Chemistry, Faculty of Science, Tanta University, Tanta 31527, Egypt

- Mitochondrial disruption: coordination compounds often trigger apoptosis by inducing mitochondrial outer membrane permeabilization (MOMP), leading to the release of proapoptotic factors such as cytochrome c.

- Death receptor activation: coordination compounds can activate death receptors (e.g., Fas, TRAIL-R1/DR4, TRAIL-R2/DR5), leading to caspase-8 activation.

- ROS generation and redox modulation: redox-active metal compounds could overcome cancer cells' antioxidant defenses by raising reactive oxygen species (ROS) levels. Oxidative stress causes damage to proteins, lipids, and DNA, which finally leads to cell death.

- Protein inhibition and functional modulation: these compounds interfere with vital signaling pathways in cancer cells by selectively inhibiting oncogenic proteins or activating tumor suppressors. They hinder survival and growth by interfering with vital biological processes, which promotes the death of cancer cells while minimizing effects on healthy tissue.

These mechanistic aspects have been explored through intensive experimental works including adopting and designing *in vitro* biochemical assays. Lately, research in developing and designing anticancer agents has suffered from overestimation, overinterpretation, and inappropriate and/or insufficient experimental data. This review aims to highlight the most important biochemical assays that can aid in understanding the possible mechanistic pathways. The methodologies, their foundation and interpretative frameworks are summarized. In doing so, we highlight promising directions for identifying the mechanistic pathways which can be facilitated in the rational design of next-generation metal-based chemotherapeutics with improved efficacy and selectivity.

## 2 Biochemical assays for anticancer drug evaluation

### 2.1 Cytotoxicity assays

The MTT assay is a widely used colorimetric assay for assessing cell metabolic activity that serves as an indirect measure of viability, and cytotoxicity, particularly in response to potential anticancer agents.<sup>13</sup> The assay relies on the ability of the metabolic activity of cells to reduce a water-soluble yellow tetrazolium salt [3-(4,5-dimethylthiazol-2-yl)-2,5-diphenyltetrazolium bromide (MTT)] into insoluble purple formazan crystals. This reaction is primarily facilitated by mitochondrial dehydrogenase enzymes which reflect the metabolic activity of living cells. The lack of enzymatic activity in dead or non-viable cells makes them unable to produce formazan (Fig. 1).<sup>14</sup> After incubation, the formazan is dissolved (with DMSO or acidic isopropanol), and absorbance is measured at 570 nm using spectrophotometry.

The procedure is established by seeding cells into a 96-well plate and allowing them to adhere and grow. After appropriate incubation, cells are treated with potential anticancer agents at various concentrations and for defined time periods (24, 36, 48 or 72 hours). The yellow MTT salt is transformed into insoluble purple formazan crystals by mitochondrial dehydrogenases in live cells after the MTT reagent is directly added to each well and incubated for one to four hours. Dimethyl sulfoxide (DMSO) or acidified isopropanol is then used to dissolve these crystals, producing a blue-colored solution. The number of metabolically active cells is directly correlated with the resulting color intensity, the intensity of which can be measured using a spectrophotometer or plate reader, and is typically in the range 540–570 nm. The outcome of the assay is



**Dalal Alezi**

*Dalal Alezi is an Assistant Professor of Chemistry at King Abdulaziz University (KAU, Kingdom of Saudi Arabia) and an Ibn Khaldun Fellow at the Massachusetts Institute of Technology (MIT). She earned her Ph.D. from the King Abdullah University of Science and Technology (KAUST) under the supervision of Professor M. Eddaoudi. Her research focuses on pioneering the design and synthesis of metal-organic*

*frameworks (MOFs) using reticular chemistry to drive transformative innovations. These materials have the potential for applications in gas storage and separation, catalysis, drug delivery, atmospheric water sorption, energy storage, and sensing. Recently, she has started focusing her research on developing metal complexes as potential anticancer candidates.*



**Abrar S. Iskandrani**

*Abrar Iskandrani holds a B.Sc. in Chemistry from King Abdulaziz University and an M.Sc. in Chemistry from the University of Jeddah, both with an Excellent Academic standing. She is currently a Ph.D. candidate in Chemistry at King Abdulaziz University, working under the supervision of Prof. Bandar Babgi and Dr Dalal Alezi. Her doctoral research focuses on the synthesis of Schiff base tridentate ligands and their*

*complexes with platinum and palladium, and the study of their anticancer activities. Abrar has contributed to teaching undergraduate chemistry courses at King Abdulaziz University since 2021.*

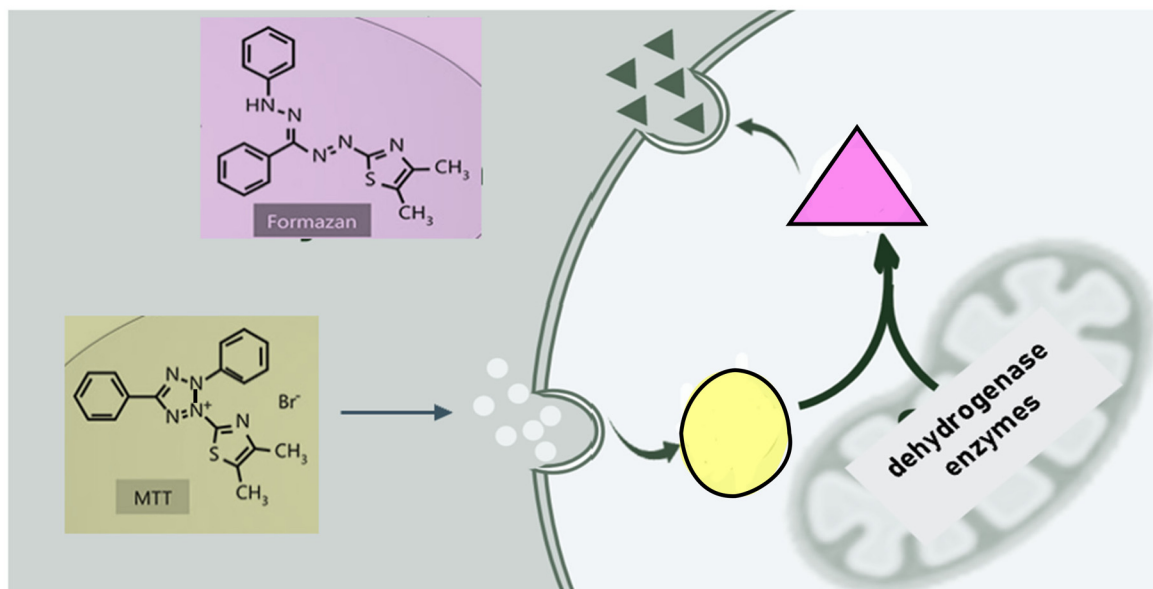


Fig. 1 Illustration of the concept of the MTT assay.

expressed as absorbance values, which directly correlate to the number of viable cells. Normalized data (against untreated control cells (100% viability)) are used to represent the findings (percent of viability). In the context of cytotoxicity studies, anticancer agents cause a decrease in absorbance indicating a reduction in cell viability, suggesting drug-induced cell death or growth inhibition. Dose–response curves can be sketched to calculate  $IC_{50}$  values (the concentration of drug that inhibits 50% of cell viability), providing a quantitative measure of anticancer

potential in the studied compound. A positive control is typically included to ensure the reliability of the data and to enable meaningful interpretation of structure–property relationships.

Despite its simplicity, the MTT assay has limitations: (1) it does not distinguish between types of cell death (apoptosis, necrosis or autophagy) and (2) the results may be influenced by drugs that interfere with mitochondrial function.<sup>15</sup> Nevertheless, it remains a foundation assay in anticancer studies for preliminary screening.



Ehab M. M. Ali

Prof. Ehab M. M. Ali is a Professor at the Department of Biochemistry, Faculty of Science, King Abdulaziz University (KAU), Saudi Arabia, a position he has held since 2018. Professor Ali got his professorship in 2010 at Tanta University, Egypt, where he previously held roles as an Assistant Professor and a Lecturer in Biochemistry. His academic career is marked by cancer biology and enzymology, with a productive research portfolio that includes 111 publications and three book chapters.

His research focuses on the development of novel compounds, formulation of therapeutic agents, and repurposing of approved drugs for alternative disease treatments. His work integrates molecular docking, computational biology, and advanced biochemical assays to explore anticancer mechanisms, drug resistance, and therapeutic innovations particularly involving metal-based complexes and natural products.



Bandar A. Babgi

Prof. Bandar A. Babgi obtained his B.Sc. in Chemistry from King Abdulaziz University in 2003. He then conducted graduate studies at the Australian National University, where he earned his M.Phil. in Chemistry in 2009 and his Ph.D. in Chemistry in 2012 under the supervision of Prof. Mark Humphrey, focusing on the development of organometallic complexes with non-linear optical properties.

Following the completion of his doctorate, he was appointed Assistant Professor in 2012, promoted to Associate Professor in 2017, and attained the rank of Professor in 2023. Prof. Babgi's research interests center on the design and synthesis of coordination and organometallic compounds, particularly those involving platinum-group metals and copper, with a strong emphasis on their photophysical, electrochemical, and anti-cancer properties.

The sulforhodamine B (SRB) assay is a colorimetric sensitive method which is used to evaluate cell density based on total cellular protein content, making it a powerful tool for assessing cell proliferation, cytotoxicity, and drug efficacy.<sup>16</sup> Unlike the MTT assay, which relies on enzymatic activity, the SRB assay measures the amount of cellular protein as a direct indicator of cell mass, offering a more stable and linear response. The principle of the assay is based on the ability of the bright pink SRB dye to bind stoichiometrically to basic amino acid residues (primarily lysine) under weak acidic conditions.

The procedure begins by plating cells in 96-well microplates and allowing them to adhere and grow. Once the cells reach the desired confluence, they are treated with chemotherapeutic agents. After an appropriate incubation period (usually 48 to 72 hours), the cells are fixed with trichloroacetic acid which precipitates proteins and anchors them to the well surface and stops all metabolic activity, preserving the cellular content. Then, the wells are washed to remove excess medium and unbound material. After that, SRB dye is added and allowed to bind to the fixed cellular proteins. After incubation, the excess dye is removed by washing with acetic acid, and the bound dye is solubilized in a basic solution. The absorbance at 510–565 nm (typically 540 nm) is measured to quantify the dye after adding 10 mM Tris base (pH 10.5) to solubilize the bound dye. The optical density (OD) is directly proportional to the total protein content (related to the number of cells in each well) (Fig. 2). Results are typically expressed as a percentage relative to the untreated cells' protein content (negative control), providing a measure of cell inhibition. In cytotoxicity testing, a reduction in absorbance relative to controls indicates that the test compound has inhibited cell proliferation or

induced cell death.<sup>17</sup> Like the MTT assay, SRB data can be used to calculate  $IC_{50}$  values to quantify the potency of anti-cancer agents. One of the advantages of the SRB assay is the low susceptibility to variations in mitochondrial function because it measures total biomass rather than metabolic activity, offering more stable and reliable data under a broad range of experimental conditions.<sup>18</sup>

## 2.2 DNA interaction assays

The plasmid DNA cleavage assay is employed to evaluate the DNA-damaging capability of potentially chemotherapeutic compounds. The principle of the assay is to monitor structural changes in a supercoiled plasmid (typically pBR322 or pUC19) when treated with anticancer agents; some compounds induce strand scission or conformational changes.<sup>19</sup> To understand the science behind this assay, the structure of plasmid DNA is a supercoiled form (Form I), which migrates faster during agarose gel electrophoresis due to its compact structure. When a single-strand break occurs, the supercoiled DNA relaxes into an open circular form (Form II), and/or double-strand breaks result in a linear form (Form III). These distinct forms can be easily detected and visualized by gel electrophoresis.<sup>20</sup>

The assay is established by mixing a fixed amount of plasmid DNA with the examined compound in a buffer solution; the presence of a cofactor is essential if oxidative damage is investigated (either a reducing agent such as ascorbic acid or an oxidizing agent such as hydrogen peroxide). The reaction mixture is incubated under physiological conditions (pH = 7.3–7.4 and  $T = 37\text{ }^{\circ}\text{C}$ ) for a fixed time (30 minutes to 4 hours). The reaction is then terminated by adding a DNA loading dye and cooling the sample. Agarose gel electrophoresis is used to separate the samples, and the gel is stained with ethidium

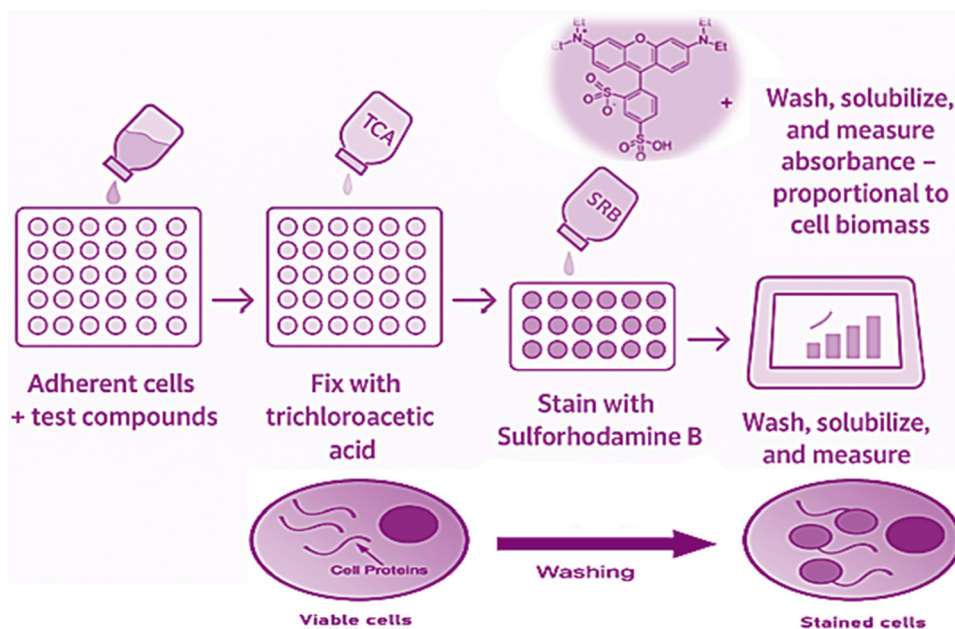


Fig. 2 Illustration of the concept of the SRB assay.

bromide or SYBR Safe (for staining) to allow visualization of the DNA bands under a UV lamp. The outcome of the assay is an image showing one or more bands corresponding to the supercoiled, open circular, and/or linear forms of the plasmid (Fig. 3). A compound that causes DNA strand breaks will show the open circular and/or linear forms' bands. Interpretation of the results provides insight into whether a compound induces direct DNA cleavage through covalent binding or oxidative stress.<sup>20</sup>

The plasmid cleavage assay is important in mechanistic studies of chemotherapeutic compounds, helping to identify agents that may function as DNA-targeting drugs. It offers a clear and direct measure of DNA interaction and damage, making it an important assay in the screening of genotoxic or DNA-active compounds.<sup>20</sup>

The Comet assay or single-cell gel electrophoresis technique is used to detect DNA strand breaks in individual cells. The core idea of the assay is the migration of fragmented DNA out of the nucleus during electrophoresis: intact DNA remains largely within the nucleus, while broken or relaxed DNA strands migrate toward the anode, forming a "tail". The extent and intensity of the tail correlate with DNA damage, making the assay useful for evaluating genotoxicity, oxidative stress, and the DNA-damaging effects of chemotherapeutic agents, including metal-based coordination compounds.<sup>21</sup>

The procedure is established by embedding cells in a thin layer of low-melting-point agarose on a microscope slide. The cells then proceed to lysis under alkaline conditions to remove membranes and proteins, leaving behind nucleoids composed of supercoiled DNA. Both single- and double-strand breaks, as well as alkali-labile sites, can be detected. After lysis, the samples are subjected to electrophoresis in a high-pH buffer. Damaged DNA migrates out of the nucleoid toward the anode, with the extent of migration depending on the number and size of DNA fragments. After that, DNA is stained with fluorescent dye such as ethidium bromide or SYBR Green, and the slides are examined under a fluorescence microscope (Fig. 4).<sup>22</sup>

The outcome of the assay is a microscopic image of each cell's DNA fragmentation pattern. Undamaged cells show

compact, rounded heads with minimal or no tail formation, while cells with increasing DNA damage exhibit progressively longer and more diffuse tails. Image analysis software can be used to quantify DNA damage by measuring parameters such as tail length, tail intensity, and tail moment which allows for comparative analysis across structurally related compounds. The Comet assay is highly valued for its sensitivity, simplicity, and capability to detect low DNA damage at the single-cell level. It is particularly useful in evaluating the genotoxic potential of the tested compounds and can be adapted for oxidative DNA damage detection by incorporating enzymes such as formamidopyrimidine DNA glycosylase (FPG).<sup>24</sup>

DNA melting studies are a fundamental method utilized to investigate the thermal stability of DNA and its adducts with interacting molecules, including potential anticancer compounds. The assay employs the thermal denaturation process (conversion of double-stranded DNA into single strands).<sup>25</sup> This process is known as melting and can be monitored by measuring the increase of absorbance (hyperchromicity) of DNA at 260 nm when the strands separate. The temperature at which half of the DNA becomes single-stranded is termed the melting temperature ( $T_m$ ), quantifying the DNA stability.<sup>26</sup>

The assay is conducted by preparing a solution by mixing a certain amount of the compound with DNA (e.g., calf thymus DNA) in buffer system (pH = ~7.3–7.4) and the mixture is gradually heated (25–95 °C) while monitoring the absorbance at 260 nm by a UV-vis spectrophotometer. A melting curve is generated by plotting absorbance *versus* temperature, and the  $T_m$  is determined as the midpoint of the transition from the low-absorbance to high-absorbance (ssDNA) state (Fig. 5). The data obtained and discussed in this assay are typically the shift in  $T_m$  value compared with free DNA. An increase in  $T_m$  suggests that the compound stabilizes the DNA helix, often through intercalation or groove binding, which strengthens base-pair interactions and hinders strand separation. Conversely, a decrease in  $T_m$  may indicate DNA destabilization, strand cleavage, or interaction that promotes unwinding. This makes DNA melting studies valuable for screening compounds that target DNA. For metal-based coordination compounds,

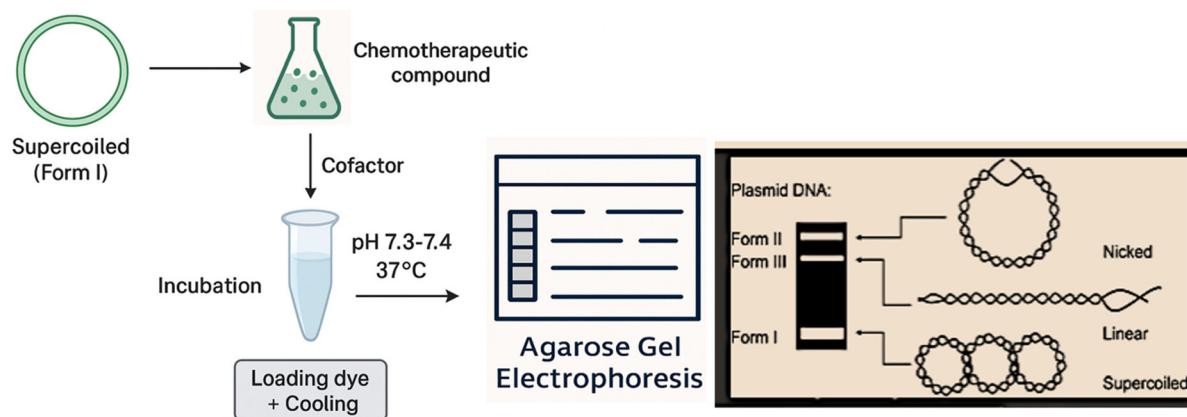


Fig. 3 Illustration of the plasmid DNA cleavage assay.

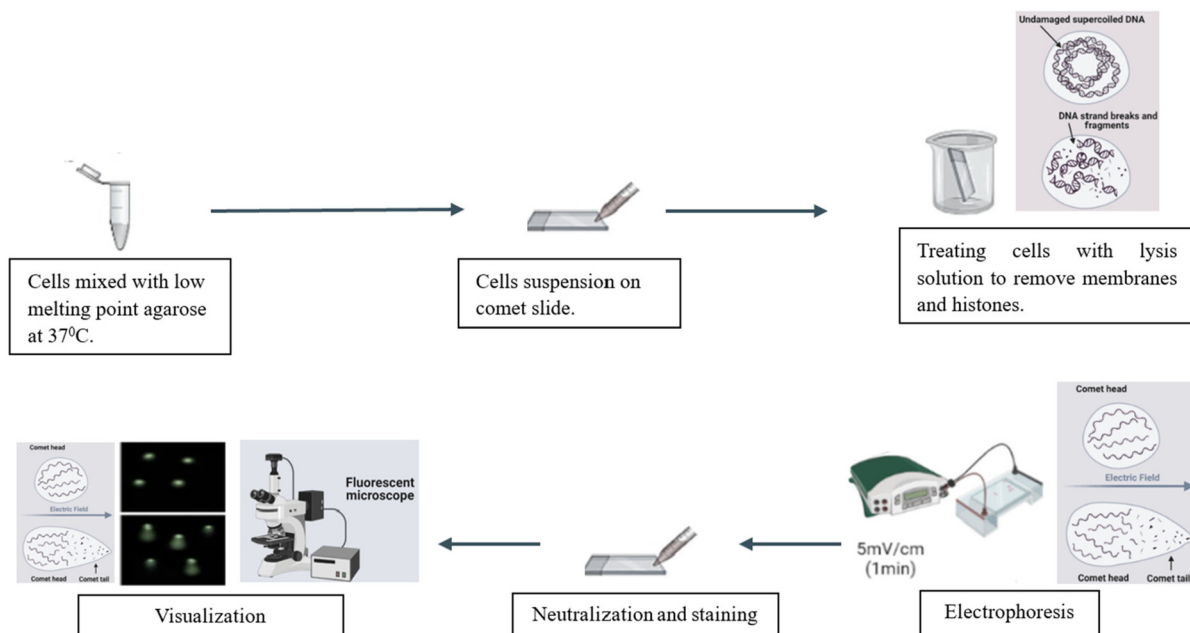


Fig. 4 Schematic representation of the Comet assay technique [modified from ref. 23 under a Creative Commons Attribution (CC BY) license, copyright 2025].

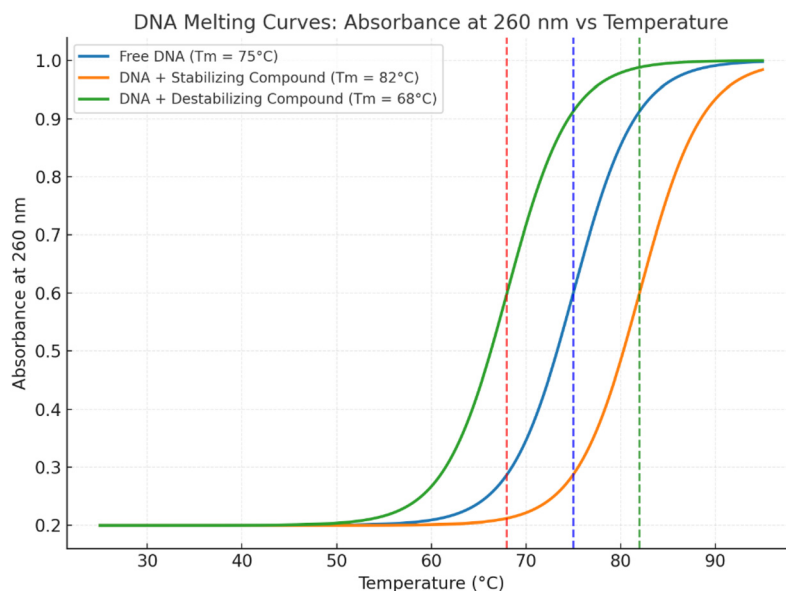


Fig. 5 Illustration of melting curves by plotting absorbance versus temperature.

changes in  $T_m$  can reflect complex–DNA binding affinity, mode of action, and potential for DNA-targeted cytotoxicity.<sup>27</sup>

Although DNA melting studies do not provide direct structural information on the mode of binding, they are often employed with other assays (e.g., gel electrophoresis or viscosity measurements) to have a complete picture of DNA interaction mechanisms. One of the advantages of this assay is the relative simplicity and high-throughput means of assessing DNA-binding strength and thermodynamic effects.<sup>27</sup>

### 2.3 Apoptosis detection assays

The Annexin V-FITC/PI staining assay is a flow cytometric technique for detecting and differentiating between early and late stages of apoptosis, as well as necrosis in cancerous cells after treatment by potent anticancer agents. The principle of the assay is using the changes in the cell membrane that occur during cell death pathways. In healthy cells, phosphatidylserine (PS) is located on the inner leaflet of the plasma mem-

brane, but during early apoptosis, it becomes externalized to the outer surface. Annexin V, a calcium-dependent phospholipid-binding protein, has a high affinity for PS and, when conjugated with a fluorescent tag such as fluorescein isothiocyanate (FITC), allows for the detection of PS exposure *via* flow cytometry or fluorescence microscopy. Propidium iodide (PI), a red-fluorescent DNA-binding agent, is impermeable for live or early apoptotic cells but penetrates cells with compromised membranes, such as those undergoing late apoptosis or necrosis.<sup>28</sup>

The assay is established by treating cultured cells with the potent anticancer compound and incubating the cells for a defined period (12 h, 24 h, 36 h, 48 h or 72 h). After treatment, the cells are harvested, washed with cold phosphate buffered saline (PBS), and suspended in an Annexin-binding buffer.

Annexin V-FITC and PI are added to the cell suspension and incubated for 20 min in the dark. The stained cells are analyzed immediately by flow cytometry. Data are plotted on a two-dimensional plot: Annexin V-FITC fluorescence on one axis and PI fluorescence on the other (Fig. 6).<sup>29</sup>

The outcome enables the classification of cells into four distinct populations: Annexin V<sup>-</sup>/PI<sup>-</sup> (viable cells), Annexin V<sup>+</sup>/PI<sup>-</sup> (early apoptotic cells), Annexin V<sup>+</sup>/PI<sup>+</sup> (late apoptotic or secondary necrotic cells), and Annexin V<sup>-</sup>/PI<sup>+</sup> (necrotic cells). An increase in the Annexin V<sup>+</sup>/PI<sup>-</sup> population following treatment indicates early apoptosis, while a shift toward Annexin V<sup>+</sup>/PI<sup>+</sup> suggests progression to late-stage apoptosis.<sup>30</sup> Annexin V-FITC/PI staining is highly acknowledged for its sensitivity and ability to distinguish between apoptosis and necrosis. For anticancer metal-based drugs, they activate apoptotic pathways

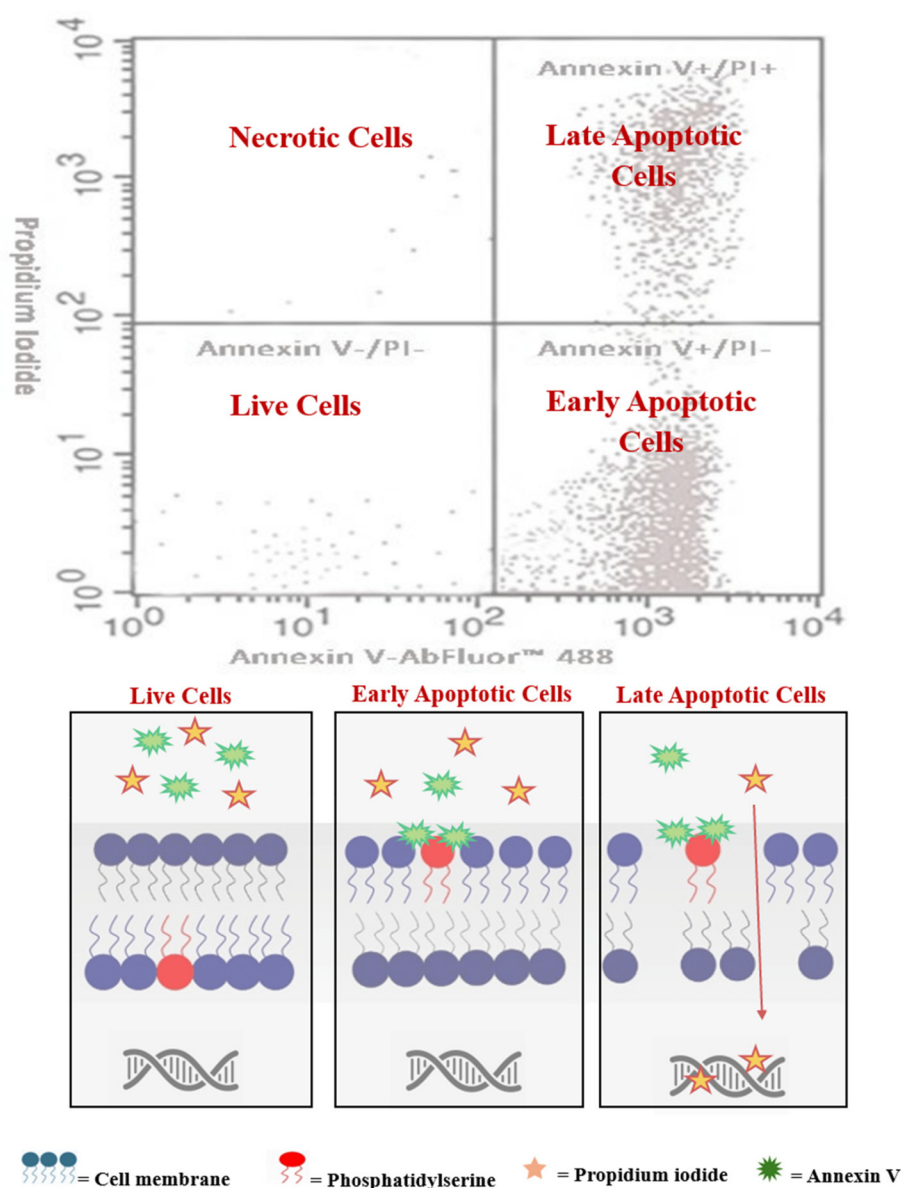


Fig. 6 The concept of the Annexin V/PI assay.

through mitochondrial disruption or ROS generation and hence this assay provides direct evidence of apoptosis induction and the mechanistic pathway.

The caspase activation assay is a key biochemical assay employed to confirm and quantify the apoptotic death pathway by detecting the activation of caspases (a family of cysteine proteases that play a central role in programmed cell death).<sup>30,31</sup> The principle of the assay relies on cleaving specific peptide substrates by active caspases, typically caspase-3, -7, -8, or -9, which are hallmarks of both intrinsic and extrinsic apoptotic pathways. These substrates are tagged with a detectable signaling moiety (chromophoric or fluorophoric) which is detectable upon cleavage (Fig. 7). Monitoring the signal spectroscopically can detect the activation of caspases due to apoptosis induction by chemotherapeutic compounds.<sup>32</sup>

The procedure typically involves treating cells with the compound of interest, and then harvesting and lysing them to collect cell extracts. A caspase-specific peptide substrate [e.g., DEVD-pNA (for caspase-3/7), IETD-AFC (for caspase-8) and so on] is added to the extract in a buffer that supports enzyme activity. The mixture is kept at 37 °C, and cleavage of the substrate is measured using a spectrophotometer (for colorimetric assays) or a fluorescence plate reader (for fluorometric assays) at appropriate wavelengths. Alternatively, some protocols allow for in-cell detection using fluorogenic caspase substrates or antibodies specific to cleaved caspases, analyzed *via* flow cytometry or fluorescence microscopy.<sup>33</sup>

The outcome of the assay is a quantitative measure of caspase activity, and the data are reported as increased absorbance or fluorescence intensity (untreated cells are used as negative controls). A significant increase in caspase activity indicates the induction of apoptosis and implicates specific caspases in the death pathway (Fig. 8). For example, activation

of caspase-9 suggests mitochondrial (intrinsic) pathway involvement, whereas caspase-8 activation points to death receptor (extrinsic) pathway initiation. Caspase-3 and -7, as executioner caspases, are typically activated downstream and are responsible for the cleavage of various cellular substrates that lead to apoptotic morphology and DNA fragmentation.<sup>34</sup>

This assay is especially valuable in mechanistic studies of anticancer agents, as it allows direct confirmation of apoptotic signaling. For metal-based coordination compounds, which often disrupt mitochondrial function or generate oxidative stress, caspase activation assays help in identifying the pathway of cell death. When used alongside assays like Annexin V/PI staining and DNA fragmentation studies, caspase assays provide robust and reliable information on apoptosis induction and progression.<sup>35</sup>

The JC-1 assay is a widely used method for assessing changes in mitochondrial membrane potential ( $\Delta\Psi_m$ ) as a crucial indicator for the intrinsic apoptotic pathway. Mitochondria maintain an electrochemical gradient across their inner membrane to produce ATP. Disruption of this gradient is one of the earliest indicators of mitochondrial-mediated apoptosis. The principle of the JC-1 assay relies on accumulation of JC-1 dye (a cationic fluorescent probe) within the mitochondria in a potential-dependent manner. In healthy cells with intact  $\Delta\Psi_m$ , JC-1 aggregates in the mitochondria, emitting red light. When the membrane potential collapses, the dye remains in its monomeric form in the cytosol, emitting green light.<sup>36</sup>

The procedure is established by incubating live cells with the JC-1 dye after treatment with the chemotherapeutic agent. After staining, the cells are washed and analyzed immediately by either fluorescence microscopy, flow cytometry, or fluorescence plate reading. The dual-emission properties of JC-1 allow for ratiometric analysis: red-to-green fluorescence ratios

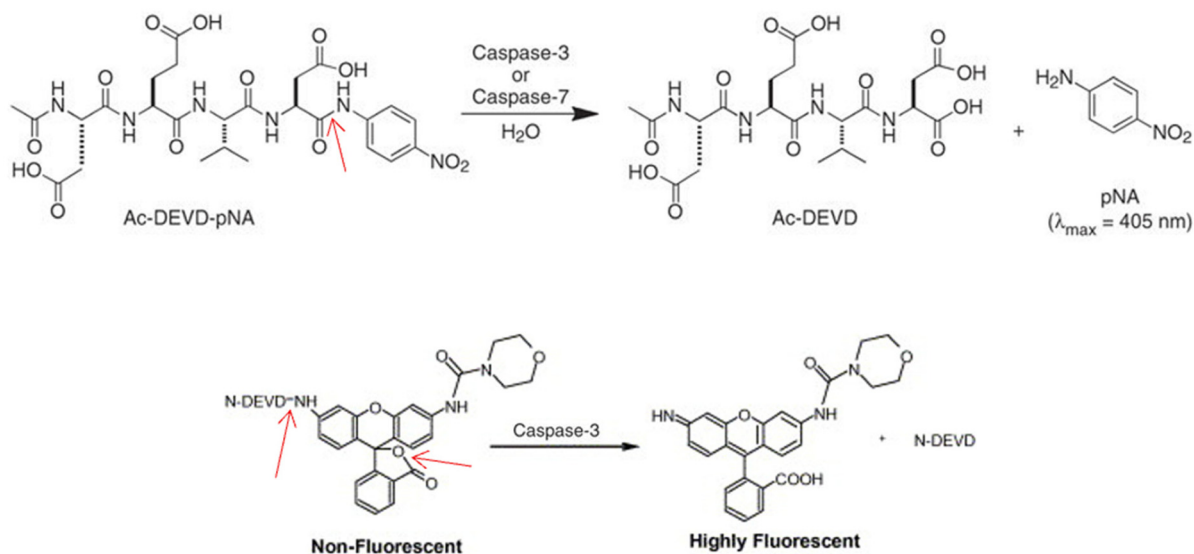


Fig. 7 Principle of caspase-3 or caspase-7 activity detection using the colorimetric method (top) or fluorometric method (bottom).

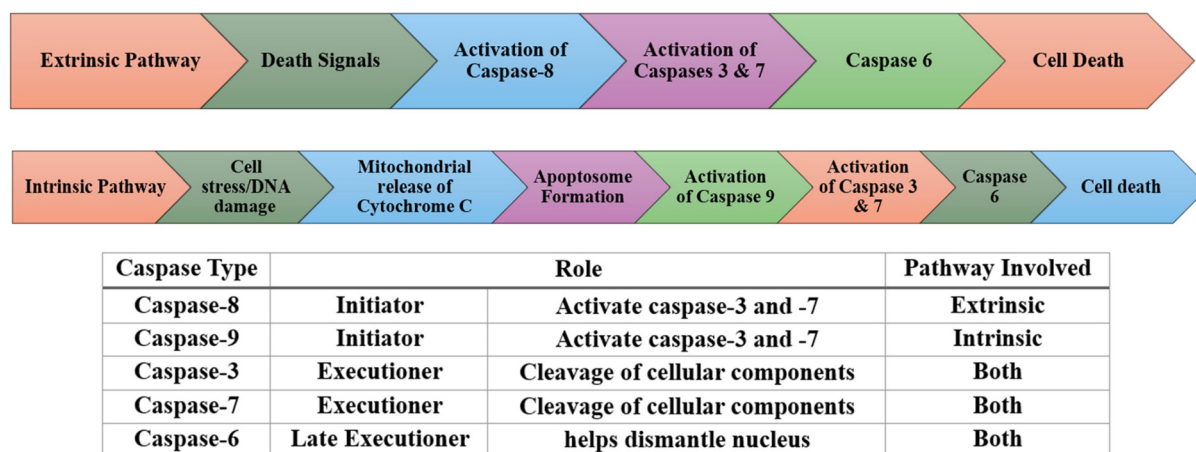


Fig. 8 Flow diagram explaining the major apoptosis pathways and the role of caspases.

provide a quantitative measure of mitochondrial health (Fig. 9). A high red/green ratio indicates polarized, healthy mitochondria, while a low ratio reflects depolarization, a hallmark of early apoptosis. The outcomes are visually and quantitatively distinct. In microscopy, healthy cells display punctate red fluorescence within the mitochondria, while apoptotic cells exhibit diffuse green fluorescence. In flow cytometry or plate-based formats, the shift from red to green fluorescence can be quantified across large cell populations. This change is often one of the earliest detectable signals of apoptosis, preceding caspase activation and DNA fragmentation.<sup>37</sup>

The JC-1 assay is valuable in the study of targeting mitochondria by metal-based chemotherapeutics. Targeting mitochondria can be either directly such as in (1) binding to mitochondrial DNA or (2) disrupting membrane proteins, or indirectly *via* (1) ROS generation or (2) oxidative stress.<sup>39</sup> Mitochondrial depolarization is a point of no return in apoptosis; hence, detecting  $\Delta\Psi_m$  collapse offers insight into the progress of cells to programmed death.<sup>40</sup> When combined with

other assays, such as caspase activity and Annexin V/PI staining, JC-1 provides a more complete understanding of the apoptotic cascade and the mechanism of action of potential anti-cancer compounds.<sup>39</sup> While JC-1 is a popular and widely used dye for assessing mitochondrial membrane potential, several other fluorescent probes such as TMRE (tetramethylrhodamine ethyl ester) and TMRM (tetramethylrhodamine methyl ester) offer viable alternatives, each with distinct advantages and limitations. TMRE and TMRM are cell-permeable, cationic dyes that accumulate in mitochondria proportional to  $\Delta\Psi_m$  and emit red fluorescence. Unlike JC-1, which requires red/green dual-emission analysis, TMRE and TMRM emit in a single channel, simplifying data acquisition and analysis. However, they require careful optimization of dye concentration and incubation time, as high concentrations can lead to mitochondrial toxicity or fluorescence quenching. One disadvantage of JC-1 is its tendency to form aggregates non-specifically or to produce ambiguous results in cells with low mitochondrial content, leading to variability. In contrast,

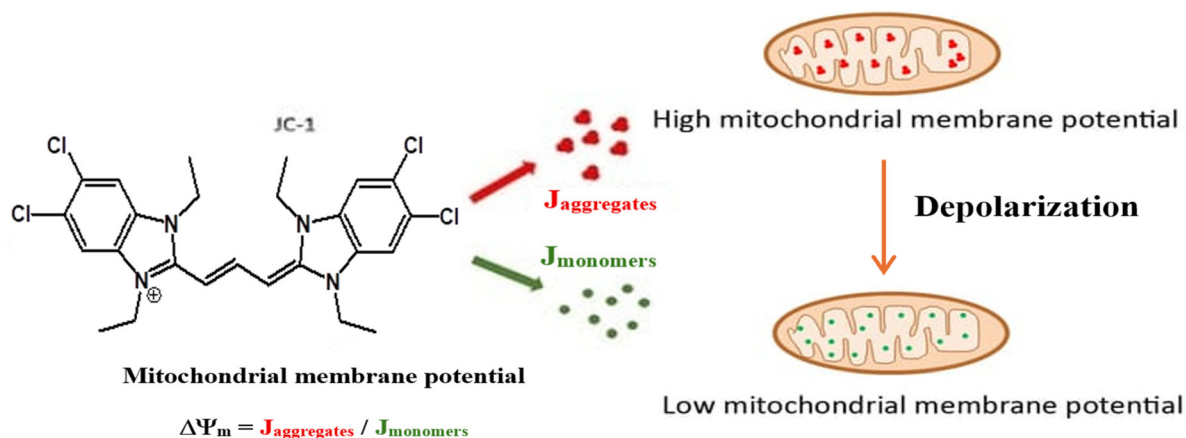


Fig. 9 The structure of JC-1 and its interactions with polarized and depolarized mitochondrial [modified from ref. 38 under a Creative Commons Attribution (CC BY) license, copyright 2025].

TMRE and TMRM offer more consistent results in sensitive cell types or under conditions where precise quantification of  $\Delta\Psi_m$  is critical. Ultimately, the choice of dye depends on the experimental context and whether qualitative imaging, precise quantification, or long-term live-cell analysis is the priority and should be guided by the dye's compatibility with the cell type, instrumentation, and downstream assays.<sup>41</sup>

## 2.4 Redox activity assays

The DCFH-DA assay is one of the commonly employed methods for detecting reactive oxygen species (ROS) within cells,<sup>42,43</sup> providing valuable insight into oxidative stress induced by chemotherapeutic agents, including metal-based coordination compounds. The principle of the assay is based on the oxidation-sensitive compound 2',7'-dichlorodihydrofluorescein diacetate (DCFH-DA). Once inside the cell, DCFH-DA is deacetylated by ROS such as hydrogen peroxide, hydroxyl radicals, and so on. DCFH is oxidized to 2',7'-dichlorofluorescein (DCF), a fluorescent compound that can be monitored by fluorescence microscopy, flow cytometry, or a plate reader ( $\lambda_{\text{EX}} = \sim 485 \text{ nm}/\lambda_{\text{EM}} = \sim 530 \text{ nm}$ ) (Fig. 10).<sup>44</sup>

The procedure involves treating cultured cells with the potential anticancer compound to induce oxidative stress, followed by incubation with DCFH-DA for 20–30 minutes at 37 °C in the dark. After washing to remove excess dye, the cells are analyzed for fluorescence intensity, which corresponds to intracellular ROS levels. The assay can be done in multi-well plates or in suspension for flow cytometry-based analysis. Some protocols also include co-treatment with known antioxidants (*e.g.*, *N*-acetylcysteine) to confirm ROS specificity.<sup>44</sup>

The outcome is measured as an increase in green fluorescence intensity, indicating elevated ROS production. In fluorescence microscopy, this appears as bright cytoplasmic fluorescence in ROS-positive cells, while flow cytometry provides

quantitative data across large populations. A significant increase in DCF fluorescence compared with untreated controls is interpreted as a rise in oxidative stress, suggesting that the test compound induces ROS generation. On the other hand, no change in fluorescence implies minimal or no ROS involvement.<sup>44</sup>

While DCFH-DA is widely used due to its simplicity and sensitivity, it has limitations. It does not distinguish between different ROS types and can sometimes be influenced by cellular redox state or autofluorescence.<sup>43</sup> Nonetheless, when interpreted alongside complementary assays (such as mitochondrial membrane potential, antioxidant enzyme activity, or caspase activation), DCFH-DA provides essential mechanistic insights into how compounds modulate oxidative stress in cancer cells.<sup>45</sup>

The glutathione (GSH) depletion assay is a method for assessing intracellular redox balance and oxidative stress, particularly in the context of studying anticancer compounds that act through reactive oxygen species (ROS) generation. GSH is a tripeptide composed of glutamate, cysteine, and glycine; it is an intracellular antioxidant that facilitates detoxifying ROS and maintains cellular redox homeostasis (Fig. 11). The principle of the assay is based on quantifying the reduced form of GSH within cells after treatment with a potential anticancer compound. A decrease in GSH levels is indicative of oxidative stress which makes this assay capable of evaluating redox-active compounds that may deplete GSH as part of their cytotoxic mechanism.<sup>46</sup>

The procedure is established by treating cultured cells with the potential anticancer compound, followed by cell lysis and protein precipitation. The GSH content in the lysate is then quantified using either a colorimetric or fluorometric method. One of the most used reagents is Ellman's reagent [5,5'-dithiobis(2-nitrobenzoic acid), or DTNB], which reacts with the thiol

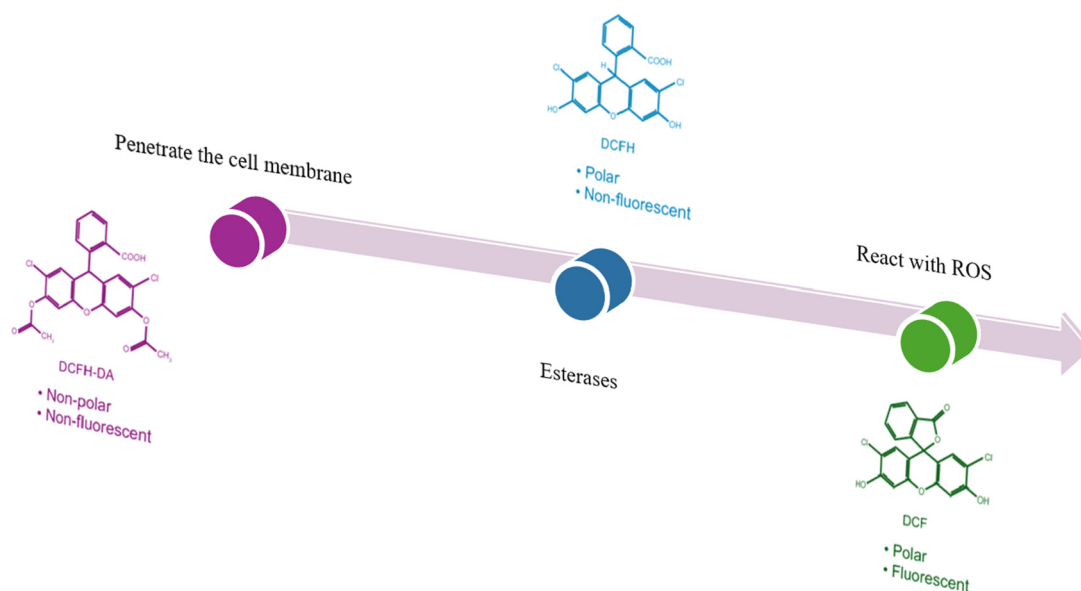


Fig. 10 Illustration of progression of DCFH-DA to DCF as a result of ROS production.

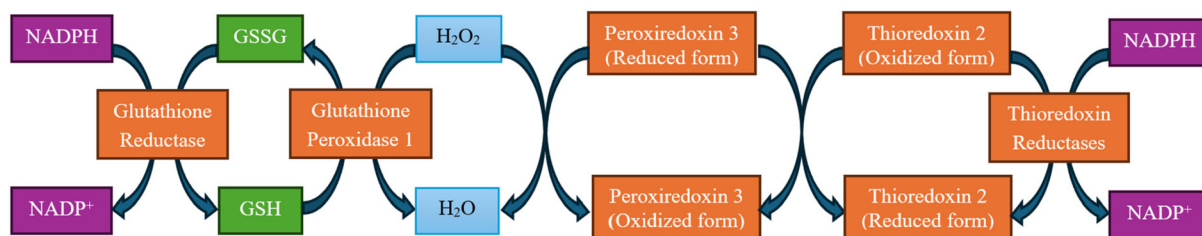


Fig. 11 The reduction of H<sub>2</sub>O<sub>2</sub> by GSH inside cells [modified from ref. 47 under a Creative Commons Attribution (CC BY) license, copyright 2025].

groups in GSH to form a yellow product TNB. TNB can be quantified by measuring the absorbance at 412 nm. Alternatively, more sensitive fluorometric kits use reagents such as monochlorobimane (MCB), which forms an emissive adduct with GSH.<sup>48</sup>

The outcome of the assay is a quantification of intracellular GSH levels, typically normalized to protein content or cell number. A significant reduction in GSH levels compared with untreated controls indicates that the compound induces oxidative stress, either by directly oxidizing GSH or by promoting ROS production that overcomes the antioxidant defense. In contrast, unchanged or elevated GSH levels suggest either low oxidative stress or an adaptive increase in antioxidant capacity.<sup>48</sup> For metal-based drugs, a decrease in GSH may also reflect direct binding or coordination between the metal center and the thiol group of the GSH, which not only depletes the antioxidant but may also affect the bioavailability and reactivity of the drug itself. While the GSH depletion assay is relatively straightforward and highly informative, it does not distinguish between reduced (GSH) and oxidized (GSSG) forms unless coupled with additional redox assays. Nevertheless, it remains a powerful tool for elucidating the redox-modulating effects of anticancer agents and for identifying oxidative stress as a potential mechanism of cytotoxicity.<sup>49</sup>

The thioredoxin reductase (TrxR) inhibition assay is a valuable method for evaluating the impact of compounds on the thioredoxin (Trx) antioxidant system which is relevant in cancer research where redox imbalance is a key therapeutic target. TrxR is a selenoenzyme that catalyzes the NADPH-dependent reduction of oxidized thioredoxin, playing a central

role in maintaining cellular redox homeostasis, DNA synthesis, and protection against oxidative stress (Fig. 12).<sup>50</sup> Many metal-based coordination compounds, especially those containing gold or platinum, are known to target TrxR by interacting with the reactive selenocysteine residue. The key point of the assay is to measure the enzyme's activity before and after treatment with a potent anticancer compound; substrates like 5,5'-dithio-bis(2-nitrobenzoic acid) (DTNB) or 9,10-phenanthrenequinone (PQ) are used to evaluate the activity of TrxR as they are subjectable to reduction, generating chromogenic or fluorogenic product.

In a typical procedure, either purified TrxR enzyme or cell lysates containing endogenous TrxR are incubated with the test compound, followed by the addition of the substrate and NADPH, the electron donor. For DTNB-based assays, TrxR activity is quantified by monitoring the increase in absorbance at 412 nm, corresponding to the formation of TNB, the reduced form. Alternatively, fluorescence-based assays using more sensitive probes like TrxR-specific activity kits or genetically encoded reporters can be employed for in-cell analysis.<sup>51</sup> The assays are usually performed in microplates, enabling high-throughput screening and dose-response analysis. The outcome is a measure of enzymatic activity, typically expressed as a percentage of activity relative to untreated controls.<sup>51</sup> A significant reduction in TrxR activity indicates enzyme inhibition, suggesting that the compound may induce oxidative stress or interfere with cellular redox regulation through TrxR targeting. This is especially relevant in cancer cells, where TrxR is often overexpressed to support rapid growth and survival. Inhibition of TrxR can lead to accumulation of ROS, mito-

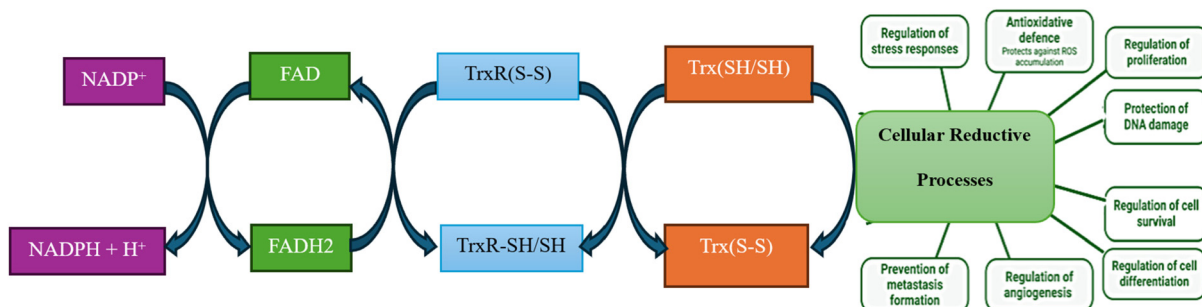


Fig. 12 The importance of thioredoxin reductase (TrxR) and the thioredoxin (Trx) systems in different cellular functions.

chondrial dysfunction, and apoptosis which make it a good target for redox-active chemotherapeutics.<sup>49</sup> Notably, metal-based compounds like auranofin (a gold(i) complex) are known TrxR inhibitors and serve as positive controls in such assays.<sup>52</sup>

While the assay is robust and informative, interpretation should consider potential off-target effects such as NADPH-dependent enzymes like glutathione reductase.<sup>53</sup> Nevertheless, TrxR inhibition assays provide a mechanistic link between redox regulation and drug action, shedding light on how anti-cancer agents leverage oxidative vulnerability in tumor cells.

## 2.5 Proteasome activity assays

They are crucial for studying the anticancer potential of coordination compounds, as proteasome inhibition is a validated strategy in cancer therapy (*e.g.*, bortezomib, a proteasome inhibitor used in multiple myeloma). Below are the key proteasome activity assays used in anticancer studies involving coordination compounds:

The fluorogenic substrate-based assay is a widely adopted method for evaluating the functional status of the proteasome, particularly the 20S core particle, which plays a pivotal role in intracellular protein turnover, stress response, and cell survival.<sup>54</sup> In cancer research, this assay is critical, as malignant cells often exhibit elevated proteasome activity to support rapid proliferation and evade apoptosis. The assay utilizes synthetic peptide substrates conjugated to fluorogenic moieties, such as 7-amido-4-methylcoumarin (AMC), which are selectively cleaved by the proteasome's active sites, chymotrypsin-like, trypsin-like, and caspase-like, generating a fluorescent signal that can be quantitatively measured. Among these, the chymotrypsin-like activity is the principal pharmacological target for proteasome inhibitors due to its dominant role in protein degradation.<sup>55</sup>

In a typical experimental setup, either purified 20S proteasome or cell lysates are incubated with fluorogenic substrates like Suc-LLVY-AMC (chymotrypsin-like), Boc-LRR-AMC (trypsin-like), or Z-LLE-AMC (caspase-like), followed by addition of the test compound and incubation under physiological conditions. Proteasome activity is then monitored by measuring fluorescence intensity, usually at excitation/emission wavelengths of 360/460 nm for AMC over time using a microplate reader. A decline in fluorescence relative to untreated controls indicates inhibition of proteasomal activity. This method is highly sensitive and supports high-throughput screening (HTS), making it ideal for evaluating the structure-activity relationships and dose-response behavior of novel anticancer agents.<sup>55</sup> While endpoint reading is common, continuous kinetic measurement (taking readings every 5–10 minutes) is highly recommended. This allows for the determination of the rate of inhibition (time-dependent *vs.* immediate), which can hint at irreversible (covalent) or reversible binding mechanisms.

Fluorogenic assays have been instrumental in the development and validation of clinically approved proteasome inhibitors such as bortezomib and carfilzomib, as well as emerging

metal-based inhibitors like gallium(III), copper(II), and gold(III) complexes, which often exhibit redox- or electrophile-mediated interactions with the proteasome's catalytic threonine residue.<sup>56</sup> Notably, this assay enables not only *in vitro* characterization but also functional studies in intact cancer cells, linking biochemical inhibition to phenotypic outcomes such as cell cycle arrest, unfolded protein response, and apoptosis. While highly robust, careful control of substrate specificity and background fluorescence is essential, especially when applied to complex biological samples. Nevertheless, the fluorogenic substrate-based proteasome assay remains a standard for investigating the mechanism of action of anticancer compounds targeting the ubiquitin–proteasome system.<sup>56</sup>

The western blot analysis of proteasome substrates is a mechanistic assay that provides qualitative and semi-quantitative evidence of proteasome inhibition by monitoring the intracellular accumulation of specific proteasome target proteins. This method is particularly relevant in cancer research, where proteasome activity is tightly linked to cell survival, proliferation, and resistance to apoptosis.<sup>57</sup> Proteins such as p27<sup>Kip1</sup>, p53, IκB-α, cyclins, and polyubiquitinated proteins are well-characterized substrates of the ubiquitin–proteasome system (UPS) and serve as biomarkers for assessing the functional status of proteasomal degradation pathways.<sup>58</sup> Upon proteasome inhibition, these substrates accumulate within the cell, providing a clear biochemical signature of impaired proteolysis either pharmacologically or genetically.<sup>57,58</sup>

In a typical protocol, cancer cells are treated with a test compound suspected to inhibit proteasomal activity, followed by lysis and protein extraction. Equal amounts of total protein are resolved *via* SDS-PAGE and transferred onto PVDF or nitrocellulose membranes. Immunoblotting is performed using specific antibodies against known proteasome substrates, including monoclonal anti-ubiquitin to detect high-molecular-weight polyubiquitinated proteins, which accumulate when the proteasome is blocked. The membrane is incubated with a primary antibody specific to the target protein. After washing, it is then incubated with a secondary antibody conjugated to an enzyme (*e.g.*, horseradish peroxidase, HRP) that recognizes the primary antibody. A substrate for the enzyme is added, producing a detectable signal (chemiluminescence, colorimetric, or fluorescent), which indicates the presence and approximate quantity of the target protein at its specific molecular weight. Additionally, increases in endogenous levels of cell cycle regulators (*e.g.*, p21, p27) or pro-apoptotic proteins (*e.g.*, Bax, NOXA) may reflect downstream effects of proteasome inhibition. The presence of loading controls, such as β-actin or GAPDH, ensures data normalization across samples.<sup>59</sup>

This assay complements fluorogenic and activity-based profiling techniques by providing cellular context and confirming that observed biochemical inhibition translates into disruption of endogenous protein degradation. Western blot analysis is especially valuable in validating the selective action of novel anticancer agents, including proteasome inhibitors like bortezomib or carfilzomib, as well as investigational compounds such as metal-based complexes or natural products.<sup>57</sup> The

accumulation of proteasome substrates is often associated with downstream events such as ER stress, unfolded protein response (UPR) activation, and apoptosis, offering mechanistic insight into how cancer cells respond to proteasome disruption.<sup>60</sup> While not quantitative in the strictest sense, this method provides visual confirmation of drug efficacy at the protein level and remains a core assay in the validation of proteasome-targeting therapeutics. However, there are a few aspects that should be considered in this assay: (A) include a well-characterized proteasome inhibitor (*e.g.*, bortezomib, MG-132) to confirm the assay is working and to compare the potency and profile of your metal-based compound and (B) ensure that accumulation is not a secondary effect of widespread cell death; it should occur at time points and doses where viability is still high (>70–80%).

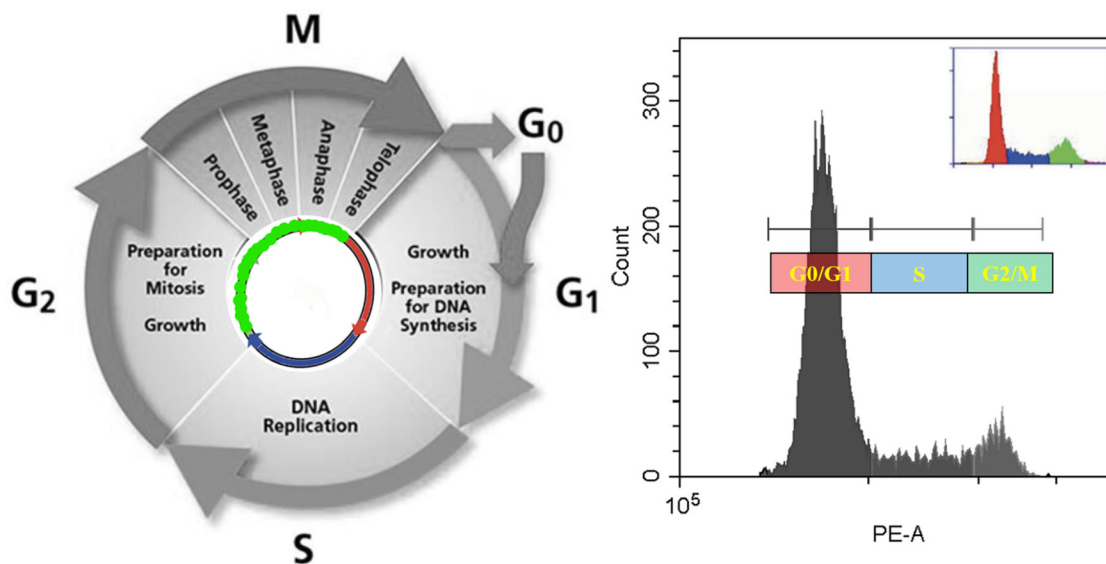
## 2.6 Flow cytometry cell cycle analysis

Flow cytometry-based cell cycle analysis is a quantitative technique used to determine the distribution of a cell population across the different phases of the cell cycle ( $G_0/G_1$ , S, and  $G_2/M$ ), providing a critical insight into how anticancer compounds, including metal-based agents, affect cellular proliferation and division. The principle relies on staining DNA with a fluorescent dye, most commonly propidium iodide (PI), which binds stoichiometrically to DNA, allowing accurate measurement of DNA content in individual cells. Cells in the  $G_0/G_1$  phase have a 2N DNA content, those in S phase are actively

synthesizing DNA and exhibit intermediate fluorescence, while  $G_2/M$  phase cells possess a 4N DNA content. Sub- $G_1$  peaks, representing cells with fragmented DNA, can also be identified and are indicative of late-stage apoptosis.<sup>61,62</sup>

The assay begins with the treatment of cultured cells with the metal-based compound of interest for a defined period (*e.g.*, 12 h, 24 h, 48 h). After treatment, cells are collected, washed with cold PBS, and fixed in cold 70% ethanol (typically overnight at  $-20\text{ }^\circ\text{C}$ ) to preserve cellular DNA and structure. Ethanol-fixed cells are then washed to remove fixative and incubated with a staining solution containing PI and RNase A. RNase A is essential to degrade RNA, ensuring only DNA is stained. The stained cells are incubated at room temperature in the dark for 30 minutes and subsequently analyzed by flow cytometry.<sup>62</sup>

Data are plotted as a histogram of PI fluorescence intensity *versus* cell count, where the peaks corresponding to the  $G_0/G_1$ , S, and  $G_2/M$  phases are resolved. Analytical software (*e.g.*, FlowJo, ModFit) is used to quantify the percentage of cells in each phase (Fig. 13). An increase in the  $G_2/M$  population may indicate DNA damage-induced arrest, as cells are unable to proceed to mitosis—this is commonly observed with metal-based drugs that target DNA (*e.g.*, platinum complexes). S-phase accumulation may suggest replication stress or inhibition of DNA synthesis, while a  $G_1$  arrest can be associated with activation of tumor suppressor pathways (*e.g.*, p53–p21 axis). Moreover, the presence of a sub- $G_1$  population is a hall-



Propidium iodide (PI) is a fluorescent dye in cell cycle analysis to measure DNA content by binding to DNA and RNA. By analyzing the fluorescence intensity of PI-stained cells using flow cytometry, researchers can determine the proportion of cells in different phases of the cell cycle ( $G_0/G_1$ , S, and  $G_2/M$ ).

- **$G_0/G_1$  phase:** Cells have a diploid DNA content (2n).
- **S phase:** Cells are actively replicating their DNA, so their DNA content is increasing from 2n to 4n.
- **$G_2/M$  phase:** Cells have duplicated DNA content (4n).

Fig. 13 Illustration of cell cycle analysis by flow cytometry.

mark of apoptotic DNA fragmentation and serves as an indirect indicator of apoptosis.<sup>63</sup>

This assay not only confirms the cytostatic or cytotoxic effects of metal-based compounds but also helps elucidate their mechanism of action, particularly when used alongside other apoptosis or DNA damage assays. For instance, if a compound induces a G<sub>2</sub>/M arrest and this coincides with  $\gamma$ -H2AX upregulation (*via* western blotting), it strongly suggests that DNA damage is the primary mechanism. Likewise, if combined with caspase activation or Annexin V positivity, a sub-G<sub>1</sub> increase reinforces evidence for apoptosis induction. Therefore, cell cycle analysis *via* flow cytometry is a powerful mechanistic tool for characterizing how metal-based agents affect cancer cell proliferation and survival.

## 2.7 Beyond the traditional biochemical assays

Understanding metal-based drug mechanisms demands a shift from DNA-focused models to a broader view of their poly-pharmacological effects. Complexes of platinum, ruthenium, gold, and titanium interact with multiple biomolecules—DNA, proteins, enzymes, and metabolites simultaneously. Recent analytical and cellular biology innovations have introduced sensitive, label-free approaches that provide holistic insight into drug–target interactions and downstream biological consequences.

**2.7.1 Mass spectrometry-based proteomics.** Mass spectrometry-based proteomics provides a comprehensive view of cellular responses to metallodrug exposure, extending beyond simple binding assays. By measuring the mass-to-charge ratio of peptide ions, high-resolution MS enables the identification of drug–protein interactions and downstream signaling alterations.<sup>64</sup> Quantitative approaches such as label-free profiling, SILAC, and isobaric tagging (*e.g.*, TMT, iTRAQ) allow multiplexed analysis of protein abundance, post-translational modifications, and pathway disruptions. This is critical for detecting off-target effects and network-level changes in cytotoxicity. The workflow involves protein extraction, enzymatic digestion (trypsin), peptide separation *via* liquid chromatography, and MS/MS analysis. Spectral data are matched to protein databases using tools like MaxQuant or Mascot, followed by quantification and statistical interpretation.<sup>64</sup> Key findings include:

- Quantitative profiling: differential abundance in treated samples highlights upregulated and downregulated proteins, such as those linked to oxidative stress or unfolded protein response (*e.g.*, heme oxygenase-1, superoxide dismutase).
- Post-translational modifications (PTM): metallodrugs influence phosphorylation, acetylation, and ubiquitination, disrupted signaling cascades.
- Pathway mapping: bioinformatics uncovers biological processes such as apoptosis, DNA repair, and metabolic regulation.

**2.7.2 Cellular thermal shift assay (CETSA).** CETSA assesses drug–target engagement in intact cells under physiological conditions by monitoring ligand-induced changes in protein thermal stability with melting point shifts indicating inter-

action.<sup>65</sup> Cells are treated with the test compound or control, and then subjected to a temperature gradient (37–65 °C) for 3 minutes to induce protein denaturation. After rapid cooling, samples are lysed in non-denaturing buffer and centrifuged to isolate soluble protein fractions. Target protein levels are quantified *via* western blotting or mass spectrometry, and thermal profiles were constructed by plotting protein abundance against temperature. A shift in melting temperature ( $T_m$ ) indicated compound-induced stabilization.<sup>65</sup> Unlike assays using purified proteins, CETSA preserves native cellular context, minimizing artifacts from cofactor loss or metal speciation. Applications include target validation (*e.g.*, TrxR1) inside cancer cells, confirmation of intracellular binding, and mechanistic insights such as caspase stabilization in apoptotic pathways.<sup>66</sup> When combined with proteomics in thermal proteome profiling (TPP), CETSA expands to a proteome-wide scale.

**2.7.3 Thermal proteome profiling (TPP).** Thermal proteome profiling (TPP) is a proteomics technique used to assess protein thermal stability and identify drug targets in living cells without requiring compound labeling in living cells. TPP is closely related to CETSA, which targets specific protein–compound interactions *via* western blotting or targeted MS, and TPP, often termed CETSA-MS, offers higher resolution and broader application.<sup>67</sup> It facilitates unbiased identification of direct and indirect drug targets, making it especially suited for multi-target agents such as metallodrugs. TPP enables comprehensive mapping of thermal shifts across thousands of proteins. TPP reveals a broad range of protein interactions, capturing both canonical targets that determine compound selectivity and noncanonical or unexpected ones, including metabolic enzymes and chaperones.<sup>67</sup>

**2.7.4 High-throughput phenotypic screening.** Automated imaging platforms with multiparametric readouts such as mitochondrial integrity, cell cycle progression, and ROS levels enable scalable phenotypic profiling. Unlike target-based assays, this approach prioritizes functional cellular outcomes, clustering compounds by similarity to known mechanisms.<sup>68</sup> The advantages of this technique include: (1) identifying the phenotypic fingerprinting: each compound yields a distinct cellular signature, facilitating mechanism prediction *via* reference library comparison; (2) capture integrated effect: it reflects multitarget and synergistic interactions often missed in reductionist assays; and (3) integrating computational methods: machine learning models enhance mechanism inference and lead prioritization.<sup>68</sup>

**2.7.5 Other label-free biophysical techniques.** Label-free methods enable direct, real-time analysis of biomolecular interactions without the need for fluorescent or radioactive tags. These techniques preserve native conformations and reduce assay complexity, making them ideal for characterizing binding kinetics, affinities, and thermodynamics. Methods for studying metallodrug interactions include: surface plasmon resonance (SPR), isothermal titration calorimetry (ITC), micro-scale thermophoresis (MST) and bio-layer interferometry (BLI) (Table 1).<sup>69–71</sup>

**Table 1** Highlights of some label-free biophysical techniques

Technique	Principle and measurement	Key strengths
SPR	Measures refractive-index shifts at sensor surface	Real-time kinetics and affinity, label-free
ITC	Detects heat changes during binding in solution	Complete thermodynamic characterization
MST	Observes changes in molecular movement due to binding in temperature gradients	Sensitive in complex matrices, very low sample amounts
BLI	Monitors optical interference <i>via</i> biosensor tips	High throughput, real-time, compatible with crude samples

## 2.8 Emerging assays for non-apoptotic cell death in metal-based cancer therapy

While apoptosis has long been considered the primary mechanism of programmed cell death induced by chemotherapeutic agents, including metal-based drugs, emerging research has revealed several alternative pathways that offer promising therapeutic opportunities. Non-apoptotic cell death mechanisms including ferroptosis, necroptosis, pyroptosis, parthanatos, and autosis are increasingly recognized as pivotal pathways in cancer biology (Table 2). Unlike classical apoptosis, which is often impaired in therapy-resistant tumors, these alternative death modalities offer distinct molecular triggers and execution mechanisms that can circumvent apoptotic resistance. Ferroptosis, for instance, is driven by iron-dependent lipid peroxidation, while necroptosis involves RIPK1/RIPK3-mediated membrane rupture, and pyroptosis is characterized by inflammasome activation and gasdermin-mediated pore formation. Parthanatos and autosis, regulated by PARP1 hyperactivation and autophagy-related processes respectively, further expand the landscape of regulated cell death. Harnessing these pathways presents a promising therapeutic strategy to selectively eliminate malignant cells that evade conventional apoptosis-inducing treatments (Table 2).<sup>72</sup> Among these, ferroptosis and necroptosis have garnered significant attention for their potential to overcome apoptosis resistance and activate distinct immunological responses within the tumor microenvironment.<sup>72</sup> Metal-based chemotherapeutic candidates, with their unique redox properties and diverse biological interactions, are particularly well-suited to induce these pathways, offering new avenues for therapeutic intervention. These pathways often engage immunogenic cell death processes, triggering inflammatory responses that can stimulate antitumor immunity and enhance the overall therapeutic outcome. For metal-based drugs, which frequently exhibit multi-target mechanisms of action, the ability to simultaneously engage multiple cell death pathways represents a particularly valuable therapeutic strategy.

### 2.8.1 Ferroptosis and its relevance to metal-based drugs.

Ferroptosis is a regulated, non-apoptotic form of cell death characterized by iron-dependent lipid peroxidation and catastrophic membrane damage. This process is initiated by the accumulation of intracellular ferrous iron ( $\text{Fe}^{2+}$ ), which catalyzes the Fenton reaction and generates reactive oxygen species (ROS). These ROS preferentially oxidize polyunsaturated fatty acids (PUFAs) within membrane phospholipids, a process

facilitated by enzymes such as ACSL4 and LPCAT3. Under normal conditions, lipid peroxides are detoxified by glutathione peroxidase 4 (GPX4), which requires glutathione (GSH) as a cofactor. Glutathione peroxidase 4 (GPX4) utilizes glutathione (GSH) to reduce lipid hydroperoxides to nontoxic lipid alcohols, thereby protecting cellular membranes from oxidative damage.<sup>72</sup> However, inhibition of GPX4—either directly (*e.g.*, by RSL3) or indirectly *via* depletion of GSH through blockade of cystine uptake by the SLC7A11/xCT antiporter—leads to unchecked lipid peroxidation. Additional regulatory pathways have recently been identified, including the FSP1-CoQ10-NAD(P)H axis, which functions as an independent parallel system to GPX4, and the GCH1-BH4 pathway that confers resistance to ferroptosis through its antioxidant properties.<sup>72</sup> The resulting oxidative damage compromises membrane integrity, culminating in cell death. Morphologically, ferroptotic cells exhibit shrunken mitochondria with dense membranes and reduced cristae, while the nucleus remains intact, distinguishing this pathway from apoptosis and necrosis. Given its unique biochemical signature and therapeutic relevance, ferroptosis represents a promising target for eliminating apoptosis-resistant cancer cells. Metal-based compounds are particularly well-positioned to induce ferroptosis due to their ability to participate in Fenton chemistry and modulate cellular iron homeostasis. Several metallodrugs have demonstrated the capacity to trigger ferroptotic death in cancer cells.<sup>83</sup> To elucidate ferroptosis mechanisms induced by metal-based compounds, several key assays are employed:<sup>84</sup>

- Lipid peroxidation assays: oxidative membrane damage (a hallmark of ferroptosis) is detected using probes such as C11-BODIPY<sup>581/591</sup> and Liperfluor, which enable real-time visualization and quantification of lipid peroxidation.

- Glutathione and GPX4 activity assays: the GSH/GSSG ratio serves as a critical indicator of redox imbalance. Luminescent or colorimetric assays distinguish reduced and oxidized glutathione, while GPX4 activity can be assessed using specific substrates (*e.g.*, phosphatidylcholine hydroperoxide). Immunoblotting for GPX4 protein levels further clarifies transcriptional *versus* post-translational regulation. Additionally, SLC7A11 expression analysis *via* cystine uptake assays or immunoblotting identifies upstream disruptions in glutathione biosynthesis—particularly relevant for gold(I/III) complexes targeting thioredoxin reductase and structurally similar selenoproteins.

- Iron metabolism assessment: given ferroptosis's iron dependency, intracellular labile iron pools are quantified

**Table 2** Cell death pathways, their characteristics and some metal-based coordination compounds known to induce it

Cell death pathway	Key morphological, biochemical events, primary inducing signal/trigger	Utilized biochemical assays	Example metal-based compound
Apoptosis	<b>Morphology:</b> cell shrinkage, membrane blebbing, nuclear fragmentation (pyknosis), apoptotic bodies. <b>Biochemistry:</b> caspase activation (caspase-3/7), phosphatidylserine (PS) externalization, cytochrome c release, DNA fragmentation. <b>Signal/trigger:</b> DNA damage, death receptor ligation, cellular stress.	Annexin V/PI staining  Caspase activity assays	Several classes of coordination compounds are known to induce apoptotic cell death.
Necroptosis	<b>Morphology:</b> necrosis-like swelling and membrane rupture but regulated. <b>Biochemistry:</b> activation of RIPK1, RIPK3, and phosphorylation of MLKL; MLKL oligomerization and plasma membrane pore formation. <b>Signal/trigger:</b> TNF $\alpha$ signaling, TLR activation, Z-DNA binding; often when caspase-8 is inhibited.	Western blot for cleaved caspases/PARP. Western blot for p-RIPK1, p-RIPK3, p-MLKL Necrostatin-1 (RIPK1 inhibitor) sensitivity assay	Several Ru(II) complexes are known to induce necroptosis. <sup>73,74</sup>
Pyroptosis	<b>Morphology:</b> rapid plasma membrane ballooning and rupture, release of pro-inflammatory content. <b>Biochemistry:</b> inflammatory caspase activation (caspase-1/4/5/11), cleavage of gasdermin D (GSDMD), N-terminal GSDMD pore formation, IL-1 $\beta$ and IL-18 maturation. <b>Signal/trigger:</b> inflammasome activation ( <i>e.g.</i> , by DAMPs, PAMPs), intracellular LPS.	LDH release assay  ELISA for IL-1 $\beta$ /IL-18  Western blot for cleaved GSDMD and caspases Sytox Green/Blue dye uptake C11-BODIPY <sup>581/591</sup>	Several Ru(III) complexes are known to induce pyroptosis. <sup>75</sup>
Ferroptosis	<b>Morphology:</b> small, ruptured mitochondria, high mitochondrial membrane density, no chromatin condensation. <b>Biochemistry:</b> iron-dependent accumulation of lipid peroxides, depletion of glutathione (GSH), inhibition of system Xc <sup>-</sup> or GPX4. <b>Signal/trigger:</b> GPX4 inhibition, GSH depletion, iron overload, lipid peroxidation.	FerroOrange  GPX4 activity assay  GSH/GSSG assay Rescue by ferrostatin-1. PAR immunofluorescence/ western blot AIF nuclear translocation assay	A wide variety of metal complexes including iridium, osmium, rhenium, and ruthenium have been shown to induce ferroptosis, particularly in the context of photodynamics. <sup>76</sup>
Parthanatos	<b>Morphology:</b> nuclear condensation, loss of membrane integrity. <b>Biochemistry:</b> hyperactivation of PARP1, massive PAR polymer formation, AIF translocation from mitochondria to nucleus, nuclear DNA degradation. <b>Signal/trigger:</b> DNA damage (especially SSBs), oxidative stress.	PARP inhibitor rescue	Few Pd(II) complexes are reported to induce parthanatos. <sup>77</sup>
Autosis	<b>Morphology:</b> unique, focal swelling of the perinuclear space, increased electron-density of the cytoplasm, plasma membrane rupture. <b>Biochemistry:</b> autophagy-dependent, but distinct from classic autophagy. Requires the Na <sup>+</sup> /K <sup>+</sup> -ATPase pump. <b>Signal/trigger:</b> extreme autophagy induction ( <i>e.g.</i> , under starvation + autophagy enhancers).	Cell death despite caspase inhibition. Electron microscopy inhibition by Na <sup>+</sup> /K <sup>+</sup> -ATPase inhibitors	To the best of our knowledge, there are no known examples where metal coordination complexes directly induce autosis.
Autophagy	<b>Morphology:</b> formation of double-membrane autophagosomes engulfing cytoplasm and organelles, fusion with lysosomes. <b>Biochemistry:</b> LC3-I lipidation to LC3-II, degradation of autophagy substrates ( <i>e.g.</i> , p62/SQSTM1), Atg protein coordination. <b>Signal/trigger:</b> nutrient deprivation, proteotoxic stress, mTOR inhibition.	Western blot for LC3-II conversion and p62 degradation GFP-LC3 puncta formation assay  Autophagic flux assays	The most studied metal complexes in this context are Ru(II) and Cu(II) complexes, with mechanisms often involving ROS generation and mitochondrial dysfunction. <sup>78,79</sup>

Table 2 (Contd.)

Cell death pathway	Key morphological, biochemical events, primary inducing signal/trigger	Utilized biochemical assays	Example metal-based compound
Immunogenic cell death (ICD)	<p><b>Morphology:</b> shares features with apoptosis/necrosis.</p> <p><b>Biochemistry:</b> surface exposure of calreticulin (CRT), release of ATP and HMGB1, type I IFN response.</p> <p><b>Signal/trigger:</b> ER stress, ROS generation, pre-apoptotic Ca<sup>2+</sup> waves.</p>	<p>Surface CRT staining (flow cytometry)</p> <p>Extracellular ATP luminescence assay</p> <p>HMGB1-release ELISA</p>	Several Ru, Au and Cu complexes have also been validated for ICD induction. <sup>80–82</sup>

using FerroOrange or calcein-AM, identifying metal compounds that elevate intracellular iron levels either through increased uptake or impaired storage. Western blot analysis of transferrin receptor, ferritin, and iron regulatory proteins (IRPs) reveals whether metal-based compounds produce modulation of iron homeostasis at both transcriptional and translational levels.

**2.8.2 Necroptosis and its induction by metal-based compounds.** Necroptosis is a programmed, caspase-independent form of necrotic cell death that targets cancer cells resistant to apoptosis.<sup>72</sup> Necroptosis is triggered by Toll-like receptor agonists or other cellular stressors (*e.g.*, TNFR1 activation) and proceeds through a defined signaling cascade involving the necrosome complex, composed of receptor-interacting protein kinases RIPK1 and RIPK3, and the mixed lineage kinase domain-like pseudokinase (MLKL). The process begins with the activation of death receptors (such as TNFR1) or pattern recognition receptors, leading to RIPK1 activation.<sup>72</sup> Upon caspase-8 inhibition, RIPK1 phosphorylates RIPK3, which in turn activates MLKL, inducing a conformational change that promotes MLKL oligomerization and translocation to the plasma membrane, forming disruptive pores that lead to osmotic imbalance, cellular swelling, and eventual membrane rupture, and release of damage-associated molecular patterns (DAMPs). This immunogenic cell death not only eliminates tumor cells but also enhances antitumor immune responses, making necroptosis a promising therapeutic strategy.<sup>72</sup> The following section briefly highlights the useful assays to detect necroptosis:<sup>85</sup>

- Phosphorylation and oligomerization assays are used to detect RIPK1, RIPK3, and MLKL phosphorylation, providing evidence of necroptosis induction by metal-based compounds. MLKL oligomerization and necrosome formation are assessed by immunoprecipitation. To confirm the involvement of the necroptotic pathway in metal compound-induced cell death, inhibitors such as Necrostatin-1 (RIPK1) and NSA (MLKL) are evaluated.

- Membrane integrity and DAMP release are assays to monitor membrane rupture using dyes (*e.g.*, propidium iodide, SYTOX Green) and time-lapse imaging can track the loss of membrane integrity in individual cells following treatment with metal-based compounds. This approach can reveal distinctive necroptotic kinetics compared with other forms of cell death. The detection of released DAMPs such as HMGB1,

ATP, and heat shock proteins through ELISA or western blotting of culture supernatants provides evidence of immunogenic cell death induction by metal-based necroptosis inducers. Ultrastructural analysis by TEM (electron microscopy) can visualize necroptotic morphology: swelling, rupture, and intact nuclei.

- Functional genetic validation comprises genetic approaches that provide the most specific validation of necroptosis pathway involvement including siRNA- or shRNA knock-down of RIPK1, RIPK3, or MLKL, which rescues cell death induced by metal-based necroptosis inducers; the other pathway includes CRISPR/Cas9 knockout of RIPK3 or MLKL and confirms the pathway specificity of metal compound-induced necroptosis.

The unique properties of metal complexes, including their redox activity, ligand exchange kinetics, and multi-target capabilities, position them ideally for exploiting this alternative cell death mechanism for therapeutic benefit. To ensure accurate mechanistic elucidation, a well-structured research plan can be implemented (Fig. 14) that systematically applies key assays to identify the correct pathway of cell death.

### 3 Data interpretation: linking assays' results to mechanisms

Interpreting the results of biochemical and cellular assays is crucial for elucidating the mechanisms of action of coordination and organometallic anticancer complexes. A multi-assay approach enables comprehensive mechanistic insights.<sup>86</sup> For instance, significant cytotoxicity observed in MTT or SRB assays, when coupled with DNA melting studies, plasmid DNA cleavage, or comet assay data, strongly suggests direct DNA interaction or damage. Further confirmation is provided by increased apoptotic markers (Annexin V/PI staining, caspase activation, JC-1 assay), linking DNA damage to intrinsic apoptosis. Elevated ROS levels detected by the DCFH-DA assay, along with GSH depletion and TrxR inhibition, point toward oxidative stress as a central mediator of cytotoxicity, particularly for redox-active metal complexes. When ROS induction is not the primary driver, direct TrxR inhibition can be inferred from enzyme assays and corroborated by downstream oxidative stress responses. Proteasome inhibition, though not directly detectable by the above assays, may be suggested by apoptosis

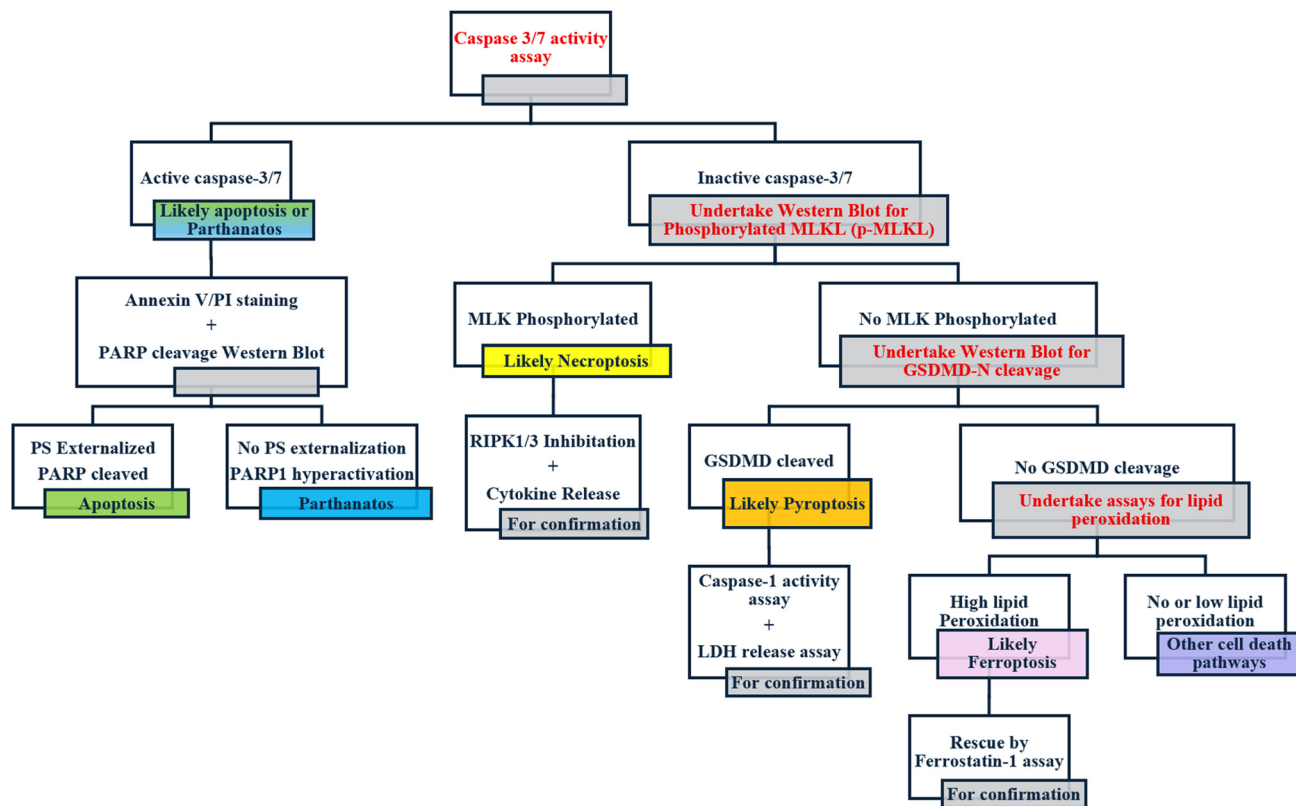


Fig. 14 A flowchart illustrating the key assays used to identify potential cancer cell death pathways.

induction independent of DNA or redox pathways and should be validated with proteasome activity assays and accumulation of ubiquitinated proteins. Thus, integration of these assays allows for precise decisions on the compound's cellular targets and downstream effects, enabling the differentiation between DNA-damaging, redox-modulating, or proteasome-inhibiting mechanisms.<sup>86,87</sup> Table 3 summarizes the concepts and data obtained from common biochemical assays. Fig. 15 illustrates how the different biochemical assays are utilized in elucidating the mechanisms of action of anticancer metal complexes.

### 3.1 Mechanism of action upon DNA binding

Covalent DNA-binding anticancer agents exert cytotoxicity primarily by disrupting DNA structure and function. DNA cross-linking agents form covalent bonds either within a single strand (intrastrand) or between complementary strands (inter-strand), impeding DNA helix unwinding.<sup>88</sup> This obstruction stalls DNA and RNA polymerases, obstructing replication and transcription, which leads to replication fork collapse and replication stress, leading to activating apoptotic cell deaths in rapidly dividing cells.<sup>89</sup>

Mechanistic validation involves multiple approaches. DNA-binding studies often show a decrease in the relative viscosity of free DNA, indicative of helix distortion or kinking. Advanced structural techniques, such as X-ray crystallography or NMR spectroscopy, can directly confirm drug–nucleobase adduct formation.<sup>90</sup> DNA melting temperature assays can reveal

increased thermal stability of DNA due to crosslinking. Flow cytometry-based cell cycle analysis typically shows S-phase arrest from replication inhibition or G<sub>2</sub>/M-phase arrest from unresolved DNA damage.<sup>89,90</sup> DNA crosslinkers promote intrinsic apoptosis, characterized by mitochondrial outer membrane permeabilization (MOMP) and activation of caspase-9 and caspase-3, which can be assessed by the JC-1 assay and caspase activity assays. Annexin V/PI staining provides further confirmation of apoptosis induction.<sup>89,90</sup>

In the case of monofunctional DNA-binding agents which form covalent adducts without crosslinking, the mechanism of cytotoxicity may involve local distortion of the DNA helix, resulting in polymerase stalling, replication fork collapse, and accumulation of single- or double-strand breaks. This class of compounds can block the transcription of survival genes or trigger apoptosis.<sup>91</sup> Although structurally distinct from classical crosslinking agents such as cisplatin or nitrogen mustards, monoadduct-forming compounds can still be highly cytotoxic, particularly when bulky lesions impede DNA replication. Mechanistic validation involves similar approaches undertaken in the case of crosslinkers.<sup>91</sup>

### 3.2 Mechanism of action upon death receptor activation

Death receptor-mediated apoptosis, also known as the extrinsic pathway, involves the activation of transmembrane receptors belonging to the tumor necrosis factor (TNF) receptor superfamily, such as Fas (CD95), TRAIL-R1 (DR4), and

**Table 3** Data from biochemical assays elucidating the mechanisms of action of anticancer metal complexes

Assay	Purpose	Mechanism(s) correlated	Important comments	Key pitfalls	How to avoid the pitfalls
MTT assay	Measures cell viability/metabolic activity <i>via</i> mitochondrial enzymes.	General cytotoxicity (indirectly supports all mechanisms).	Common screening tool but not mechanistically specific.	Precipitate insolubility; cellular reduction variability.	Ensure complete solubilization; control for cell number/metabolism.
SRB assay	Quantifies total protein content (cell density) for cell proliferation.	General cytotoxicity (supports all mechanisms).	More stable than MTT; not affected by mitochondrial redox status.	Inconsistent dye binding; incomplete washing.	Fix cells properly; standardize washing and drying steps.
Plasmid DNA cleavage assay	Assesses DNA strand breakage potential by the compound.	DNA binding and damage.	<i>In vitro</i> test; does not reflect nuclear uptake or chromatin structure.	Nuclease contamination; ambiguous supercoiled/linear forms.	Use sterile techniques; include proper controls (no drug, enzyme).
Comet assay	Detects DNA damage at the single-cell level.	DNA binding and damage, ROS generation.	Sensitive to DNA breaks caused by redox or direct interaction.	DNA damage from handling; high background.	Gentle cell handling; run in dark; include controls.
DNA melting studies	Measures changes in DNA thermal stability ( $\Delta T_m$ ) upon ligand binding.	DNA binding and damage.	Indicates DNA intercalation/groove binding strength.	Buffer effects; incorrect concentration.	Use cacodylate or phosphate buffer; ensure pure, correct DNA conc.
Annexin V-FITC/PI assay	Detects early (Annexin V) and late (Annexin/PI) apoptosis.	Mitochondrial disruption, death receptor activation, protein inhibition.	Does not distinguish between intrinsic/extrinsic apoptosis pathways.	Early apoptosis vs. necrosis confusion; timing critical.	Use unstained and single-stained controls; analyze immediately.
Caspase activation assay	Detects activity of caspases ( <i>e.g.</i> , caspase-3, -8, -9).	Death receptor activation (caspase-8), mitochondrial disruption (caspase-9), protein modulation.	Important to identify specific apoptotic pathway; should be isoform-specific.	Non-specific cleavage; activity loss.	Include inhibitor control; use fresh lysates; follow protocol times.
JC-1 assay	Assesses mitochondrial membrane potential ( $\Delta\Psi_m$ ).	Mitochondrial disruption.	Loss of $\Delta\Psi_m$ indicates mitochondrial outer membrane permeabilization (MOMP).	Artifacts from over-staining; photobleaching.	Titrate dye concentration; protect from light.
DCFH-DA assay	Measures intracellular reactive oxygen species (ROS).	ROS generation and redox modulation.	May require controls to confirm ROS origin (mitochondrial vs. non-mitochondrial).	Auto-oxidation; non-specific oxidation.	Include ROS scavenger control; protect from light; minimize assay time.
GSH depletion assay	Quantifies glutathione (GSH) levels, a key antioxidant.	ROS generation and redox modulation.	Depletion suggests oxidative stress or redox imbalance.	Rapid GSH oxidation; reagent instability.	Prepare reagents fresh; deproteinize samples quickly.
TrxR inhibition assay	Measures thioredoxin reductase (TrxR) activity.	ROS generation and redox modulation, protein inhibition	TrxR is often overexpressed in tumors; inhibition leads to redox imbalance	Non-specific DTNB reduction; enzyme instability.	Include no-enzyme control; use fresh enzyme aliquots.
Proteasome activity assay	Quantifies chymotrypsin-like activity of the proteasome.	Protein inhibition and functional modulation.	Specific for compounds that block proteasomal protein degradation.	Cytosolic protease interference.	Use specific inhibitors ( <i>e.g.</i> , lactacystin) as controls.
Western blot ( <i>e.g.</i> , $\gamma$ -H2AX, p53)	Detects specific proteins or post-translational modifications.	DNA damage ( $\gamma$ -H2AX), protein inhibition ( <i>e.g.</i> , p53 activation, caspase cleavage).	Highly informative for validating mechanistic targets.	Non-specific bands; phospho-epitope sensitivity.	Validate antibodies; use phosphatase inhibitors.
Flow cytometry cell cycle analysis	Determines distribution of cells across G <sub>0</sub> /G <sub>1</sub> , S, and G <sub>2</sub> /M phases based on DNA content.	DNA binding and damage, protein inhibition and functional modulation.	G <sub>2</sub> /M arrest suggests DNA damage; S-phase accumulation may indicate replication stress.	Doublet artifacts; sub-G <sub>1</sub> debris.	Use singlet gating; filter cells; include RNase A.

TRAIL-R2 (DR5). Upon ligand binding or compound-mediated activation, these receptors form the death-inducing signaling complex (DISC), which recruits and activates caspase-8. Active caspase-8 can directly cleave and activate caspase-3, leading to apoptosis, or cleave Bid to tBid, linking the extrinsic and intrinsic pathways by promoting MOMP.<sup>92,93</sup>

Validation of this mechanism involves caspase-8 activity assays to detect early extrinsic apoptosis. Western blotting can confirm DISC component activation (*e.g.*, Fas, FADD, caspase-8 cleavage), while Annexin V/PI staining provides apoptosis confirmation. When caspase-8 is activated independently of caspase-9, it suggests a death receptor-driven mechanism.

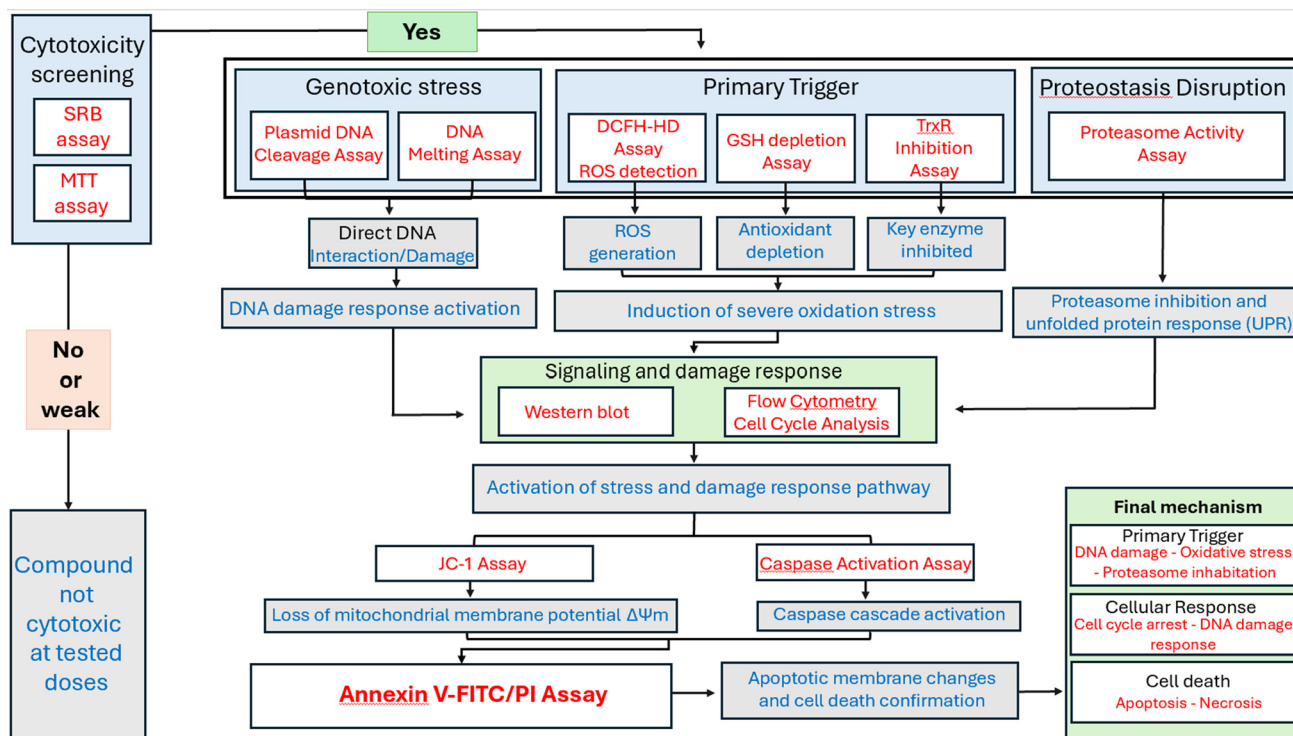


Fig. 15 Flow diagram illustrating the logic of choosing the assays to validate the mechanism of action in apoptotic cell death.

Additionally, flow cytometry can reveal changes in the surface expression of death receptors or early apoptotic markers.<sup>94</sup>

Certain metal complexes, including arsenic trioxide, gold complexes, and platinum(IV) prodrugs, have been reported to enhance death receptor expression or sensitize cells to TRAIL-mediated apoptosis. These compounds may indirectly increase receptor activity by modulating redox balance, upregulating transcription factors (e.g., CHOP, p53), or inhibiting NF- $\kappa$ B, which suppresses Fas/TRAIL signaling. Activation of extrinsic apoptosis by metal-based compounds is particularly effective in cancers with defective mitochondrial pathways, offering a complementary route to trigger cell death.<sup>95</sup>

### 3.3 Mechanism of action upon TrxR inhibition

Inhibiting TrxR blocks the regeneration of reduced thioredoxin (Trx), a key cellular antioxidant. This leads to the accumulation of reactive oxygen species (ROS) such as hydrogen peroxide and superoxide. Elevated ROS levels cause oxidative damage to lipids, proteins, and DNA, pushing cells into a state of redox imbalance.<sup>96</sup>

The resulting oxidative stress disrupts mitochondrial membrane potential ( $\Delta\Psi_m$ ), leading to the release of cytochrome c and other pro-apoptotic factors into the cytosol. This initiates the intrinsic apoptotic pathway, activating caspase-9 and caspase-3. Concurrently, ROS upregulate pro-apoptotic proteins (e.g., Bax, Bak) and suppress anti-apoptotic proteins (e.g., Bcl-2), shifting the redox balance toward cell death. Beyond apoptosis, TrxR inhibition affects DNA synthesis and repair, causes cell cycle arrest (typically at G<sub>1</sub> or G<sub>2</sub>/M), and sup-

presses redox-sensitive transcription factors such as NF- $\kappa$ B and AP-1, weakening cell survival signaling. In cancer therapy, TrxR inhibitors are valuable as they enhance DNA damage caused by chemotherapeutic agents and sensitize tumor cells to radiation, due to compromised antioxidant defenses.<sup>97</sup>

Several compounds are known to inhibit TrxR, often through direct interaction with its selenocysteine active site, making them promising anticancer agents. Auranofin, a clinically approved gold(I) phosphine compound, is one of the most well-characterized TrxR inhibitors. It selectively targets TrxR over other thiol-based reductases, leading to ROS accumulation and apoptosis in cancer cells, particularly those with high oxidative stress. Several gold(III) and gold(I) coordination complexes have shown broad-spectrum anticancer activity, often through irreversible inhibition of TrxR, mitochondrial dysfunction, and activation of cell death pathways. These compounds leverage the unique reactivity of metal centers to selectively interfere with redox enzymes in cancer cells, making TrxR an attractive target for metal-based drug design.<sup>98</sup>

### 3.4 Mechanism of action upon mitochondrial disruption

Mitochondria play a central role in the intrinsic (mitochondrial) apoptotic pathway. Many metal-based coordination compounds induce cytotoxicity by disrupting mitochondrial integrity, particularly by triggering mitochondrial outer membrane permeabilization (MOMP). This leads to the release of apoptogenic factors such as cytochrome c, Smac/DIABLO, and AIF (apoptosis-inducing factor) into the cytosol. Once released,

cytochrome c binds to Apaf-1 and procaspase-9, forming the apoptosome and activating caspase-9, which then cleaves and activates caspase-3, executing apoptosis.<sup>99</sup>

Mechanistic evaluation of mitochondrial disruption often begins with the JC-1 assay, which assesses changes in mitochondrial membrane potential ( $\Delta\Psi_m$ ). Healthy mitochondria accumulate JC-1 aggregates, emitting red fluorescence, whereas depolarized mitochondria contain JC-1 monomers, which fluoresce green. A shift from red to green fluorescence indicates MOMP.<sup>100</sup> Caspase-9 and caspase-3 activity assays further validate the activation of intrinsic apoptosis,<sup>101</sup> while Annexin V/PI staining supports apoptosis detection by confirming phosphatidylserine externalization and membrane integrity loss.

Some metal-based agents, particularly gold(I/III), copper(II), and ruthenium(II) complexes, accumulate in mitochondria due to their lipophilic or cationic nature. These compounds interfere with the mitochondrial electron transport chain, generate mitochondrial ROS, or bind directly to thiol-containing mitochondrial enzymes, resulting in MOMP. Mitochondrial dysfunction also disrupts ATP production and calcium homeostasis, amplifying cellular stress. Thus, targeting mitochondria is a powerful and selective strategy for inducing cancer cell death, especially in apoptosis-resistant tumors.<sup>102</sup>

### 3.5 Mechanism of action upon ROS induction

Reactive oxygen species (ROS)-inducing agents work by disrupting the intracellular redox balance and causing oxidative stress, which selectively harms cancer cells already under elevated metabolic strain. Excess ROS react with vital biomolecules, leading to DNA strand breaks and base modifications (e.g., 8-oxoG), lipid peroxidation that disrupts membrane integrity, and protein oxidation that impairs enzyme activity and signal transduction. This biochemical damage causes widespread cellular dysfunction and activates stress signaling pathways that ultimately lead to apoptosis or necrosis.<sup>103</sup>

One of the earliest consequences of ROS overload is the loss of mitochondrial membrane potential ( $\Delta\Psi_m$ ), which promotes mitochondrial outer membrane permeabilization (MOMP). This allows the release of pro-apoptotic factors such as cytochrome c and Smac/DIABLO into the cytosol, triggering caspase-9 and caspase-3 activation and initiating the intrinsic apoptotic pathway. In parallel, oxidative stress activates kinases like MAPK (JNK, p38) and ASK1, which upregulate pro-apoptotic genes (Bax, PUMA) and suppress anti-apoptotic ones (Bcl-2). The tumor suppressor p53 is also activated under oxidative conditions, contributing to cell cycle arrest and apoptosis. Some ROS-inducing agents act by disrupting antioxidant systems, such as glutathione (GSH) depletion, or inhibition of thioredoxin reductase (TrxR) and superoxide dismutase (SOD). This collapse of cellular redox buffering further sensitizes cancer cells to oxidative damage. When apoptosis is blocked or insufficient, ROS can induce alternate cell death pathways like ferroptosis (lipid peroxidation-driven, iron-dependent), necroptosis (regulated necrosis *via* RIPK1/3 and MLKL), or

other forms like autophagy or parthanatos, depending on cell context and ROS levels.<sup>103</sup> Several classes of compounds are known to exert anticancer activity through ROS generation. Copper(II) and iron(III) coordination complexes can catalyze Fenton-like reactions, producing highly reactive hydroxyl radicals from intracellular hydrogen peroxide. These reactions cause site-specific oxidative damage to DNA and other cellular components. Additionally, organoselenium and organotellurium compounds disrupt redox homeostasis by modifying thiol groups or interfering with enzymes like TrxR and glutathione peroxidase, leading to sustained ROS buildup. These agents are particularly effective in exploiting the already stressed redox environment of cancer cells, making them promising candidates for redox-targeted therapy.<sup>102</sup>

### 3.6 Mechanism for apoptosis induction action upon proteasome inhibition at the $\beta 5$ subunit

Proteasome inhibitors exert their anticancer effects by selectively blocking the chymotrypsin-like activity of the  $\beta 5$  subunit within the 20S core of the proteasome—an essential protein degradation complex in eukaryotic cells responsible for cleaving peptide bonds at the C-terminal side of hydrophobic residues. This inhibition leads to the accumulation of polyubiquitinated proteins, disrupting the normal turnover of key regulators such as cell cycle proteins (p21, p27, cyclins) and pro-apoptotic factors. The intracellular buildup of these undegraded proteins induces proteotoxic stress, triggering apoptosis (Fig. 16).<sup>104</sup>

Overloaded with misfolded proteins, the endoplasmic reticulum (ER) activates the unfolded protein response (UPR) through stress sensors like PERK, IRE1, and ATF6. If the UPR becomes excessive or prolonged, it results in the shutdown of general protein translation, induction of the pro-apoptotic factor CHOP, and mitochondrial damage. Simultaneously, inhibition of proteasomal degradation stabilizes tumor-suppressor and apoptotic proteins such as p53, Bax, and Bid, further shifting the cell toward intrinsic apoptosis. Additionally, proteasome inhibition disrupts the NF- $\kappa$ B survival pathway. Under normal conditions, the proteasomal degradation of I $\kappa$ B $\alpha$ , a key inhibitor of the transcription factor NF- $\kappa$ B, permits NF- $\kappa$ B to translocate into the nucleus. This regulated degradation serves as a pivotal step in NF- $\kappa$ B activation (Fig. 16). Normally, I $\kappa$ B $\alpha$ , an inhibitor of NF- $\kappa$ B, is degraded by the proteasome to allow NF- $\kappa$ B nuclear translocation. When degradation is blocked, NF- $\kappa$ B remains inactive, reducing the expression of survival genes like Bcl-xL, XIAP, and VEGF, and thereby suppressing cell survival and angiogenesis. The resulting cascade—proteotoxicity, UPR, mitochondrial depolarization, and caspase-9 and caspase-3 activation—leads to programmed cell death. In some cancer cells, extrinsic apoptosis (e.g., *via* Fas/FasL pathways) may also be activated.<sup>105</sup> Several metal-based compounds have been shown to inhibit the proteasome, often by targeting thiol groups or generating oxidative stress. Gold(I) and gold(III) complexes, such as auranofin, inhibit proteasome function and induce ER stress, contributing to their anticancer activity. Copper(II) and platinum(IV)

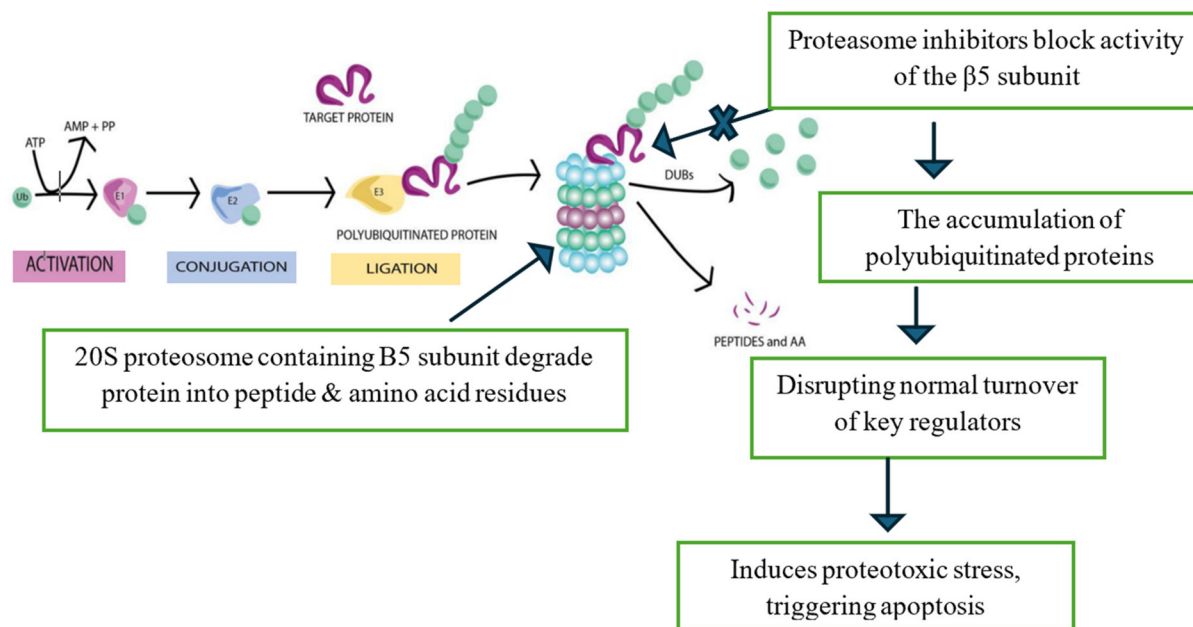


Fig. 16 Proteasome-mediated protein degradation pathway and the mode of action of proteasome inhibitors.

complexes disrupt proteasomal activity either through direct coordination with proteasome subunits or by generating redox stress that impairs its function. Another notable example is disulfiram (an aldehyde dehydrogenase inhibitor) combined with copper(II), which forms Cu-DSF complexes that inhibit both proteasome activity and NF- $\kappa$ B signaling, showing potent cytotoxicity in various cancers. These compounds exploit the reliance of tumor cells on heightened proteasome function, making proteasome inhibition a powerful strategy in anti-cancer drug design.<sup>106</sup>

### 3.7 Mechanism of action by protein targeting

In addition to directly damaging DNA or mitochondria, metal-based compounds can exert anticancer activity by selectively modulating signaling proteins and enzymes critical for tumor survival and proliferation. This mechanism involves the inhibition of oncogenic proteins (*e.g.*, kinases, transcription factors, redox enzymes) or activation of tumor suppressors (*e.g.*, p53, PTEN). These functional interferences disrupt multiple processes including cell cycle progression, DNA repair, angiogenesis, and immune evasion.<sup>107,108</sup>

Experimental validation typically involves western blotting to monitor changes in expression or phosphorylation of target proteins (*e.g.*, p53 upregulation, Akt/mTOR inhibition). Flow cytometry cell cycle analysis reveals checkpoint arrest, often at G<sub>1</sub> (*via* p21/p27) or G<sub>2</sub>/M (*via* DNA damage or microtubule destabilization). Additionally, specific activity assays (*e.g.*, for kinases, histone deacetylases, or TrxR) confirm enzymatic inhibition. Functional modulation may also manifest as differentiation, senescence, or autophagy, depending on the cellular context.

A range of metal compounds modulate protein function through various strategies. Gold(I) compounds target thiol-

and selenol-containing enzymes like thioredoxin reductase (TrxR). Copper and ruthenium complexes inhibit kinases or epigenetic modifiers (*e.g.*, HDACs), while iridium and palladium complexes show selective protein binding *via* coordination to histidines or cysteines. By bypassing conventional DNA damage routes, protein-targeting metal drugs may avoid resistance mechanisms and offer new avenues for precision therapy.<sup>109</sup>

## 4 Chemical structures and validation of mechanism of actions

The current section emphasizes the importance of undertaking multiple assays to evaluate the mechanism properly; the structural similarities between coordination compounds is not always dictating the same mechanistic pathway. For instance, Suntharalingam *et al.* (2013)<sup>110</sup> described a platinum(II) terpyridine complex (**1** in Fig. 17) that binds to DNA *via* non-covalent minor-groove association, with a measured binding constant of  $\sim 6 \times 10^4 \text{ M}^{-1}$  (*via* UV-Vis titration, FID assays, and CD) and computational docking supporting exclusive minor groove affinity and no DNA cleavage or adduct formation. Cellular uptake experiments confirmed nuclear localization, yet long-term exposure did not result in covalent adducts or DNA nicking, distinguishing it from the classical mode of cisplatin. Instead, cell death proceeded *via* a necrotic phenotype as shown by immunoblotting and DNA flow cytometry assays, without the hallmarks of genotoxic stress or apoptosis typically seen with cisplatin-induced DNA crosslinks. In contrast, cisplatin's mechanism relies on aquation-triggered covalent binding to DNA (mainly 1,2-intrastrand adducts at guanine),

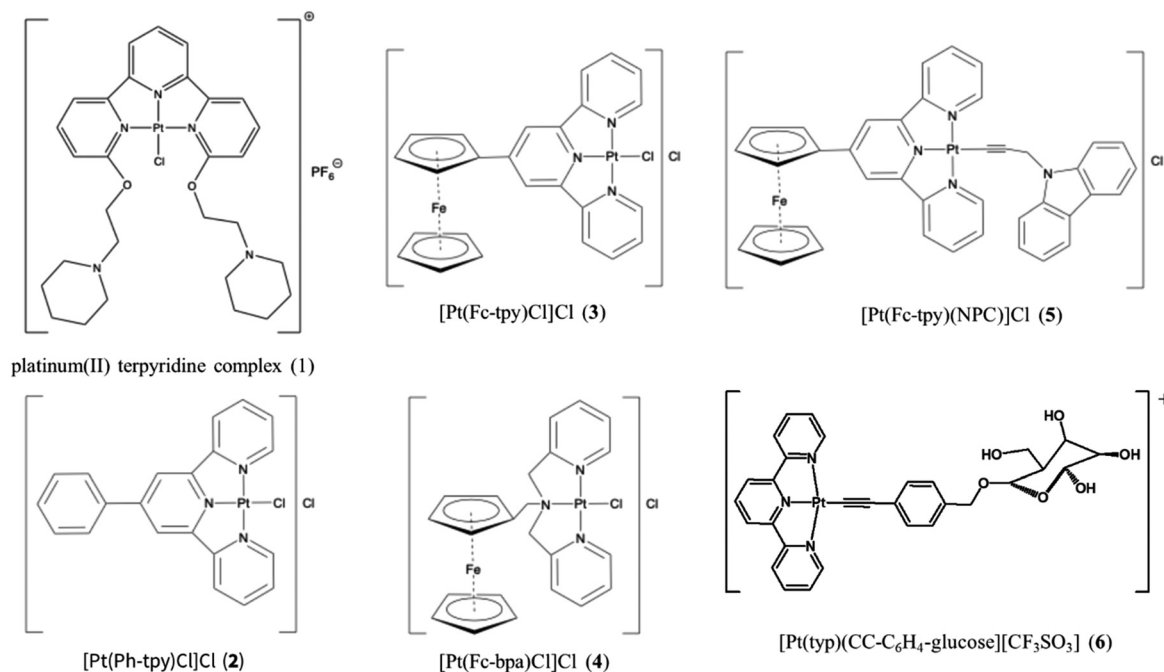


Fig. 17 Structures of different platinum complexes discussed in section 4.

transcription/replication arrest, DNA damage response (e.g.  $\gamma$ -H2AX), cell cycle arrest, and p53-dependent apoptosis. Thus, while both agents interact with genomic DNA, the terpyridine complex operates through non-genotoxic, groove-binding modalities that bypass DNA crosslink formation and initiate necrosis rather than apoptosis, marking a mechanistic departure from cisplatin's canonical pathway.<sup>110</sup> In another work, Mitra *et al.* (2014)<sup>111</sup> synthesized four platinum(II) complexes featuring ferrocenyl-terpyridine ligands (2–5 in Fig. 17) and investigated their light-activated anticancer properties. Complexes [Pt(Fc-tpy)Cl]Cl (3) and [Pt(Fc-tpy)(NPC)]Cl (5) exhibited potent photocytotoxicity under visible light ( $IC_{50} \sim 9.8$  and  $12.0 \mu M$ , respectively) with minimal dark toxicity ( $IC_{50} > 60 \mu M$ ), attributed to ROS generation *via* photoinduced oxidation of the ferrocenyl moiety. The resulting ferrocenium ions triggered Fenton-type reactions producing cytotoxic hydroxyl radicals, establishing oxidative stress as the main mechanism of action. Apoptosis was confirmed by Annexin V-FITC/PI staining and DNA fragmentation assays following light exposure. Although both 3 and 5 showed DNA binding in UV-vis titration and cellular localization studies revealed nuclear and cytoplasmic accumulation,  $\gamma$ -H2AX or comet assays were not conducted, and no significant DNA damage was reported in the absence of light, suggesting that DNA interaction was not the primary cytotoxic trigger. Complex [Pt(Fc-bpa)Cl]Cl (4) displayed DNA binding and cellular uptake but lacked the strong absorption necessary for ROS induction, resulting in low photocytotoxicity. The control compound [Pt(Ph-tpy)Cl]Cl (2), which lacks the redox-active ferrocenyl group, also bound DNA but showed no photocytotoxic effect, confirming that ROS generation, not DNA binding, was the critical factor. These results support an

ROS-mediated mechanism of action upon light activation for compounds 3 and 5, leading to apoptotic cell death.<sup>111</sup> Tong *et al.* (2021)<sup>112</sup> developed a glucose-functionalized platinum(II) acetylide complex (6 in Fig. 17) capable of dynamic supramolecular self-assembly in aqueous media. The complex exhibited potent cytotoxicity in lung cancer cell lines, attributed to its disruption of the autophagy-lysosomal pathway and subsequent mitochondrial dysfunction. Cellular uptake studies indicated endocytic internalization with lysosomal accumulation, where acidic cleavage activated the cytotoxic species. JC-1 assay revealed a significant loss of mitochondrial membrane potential ( $\Delta\Psi_m$ ), consistent with mitochondrial outer membrane permeabilization. Disruption of lysosomal integrity was confirmed by LysoTracker staining and release of cathepsins into the cytosol, while increased LC3-II levels and accumulation of autophagosomes indicated autophagic flux perturbation. Despite UV-vis evidence of potential DNA interaction,  $\gamma$ -H2AX staining showed negligible DNA damage, suggesting that cell death was driven primarily by lysosomal destabilization and mitochondrial impairment rather than genotoxicity.<sup>112</sup>

## 5 Illustration of mechanistic validation in the literature

Angelico D. Aputen *et al.* (2023)<sup>113</sup> synthesized novel platinum(IV) prodrugs featuring indole-derived axial ligands. Among these, some complexes showed potent cytotoxicity in cancer cell lines *via* ROS generation, leading to mitochondrial disruption and triggering intrinsic apoptosis in cancer cells.

DCFH-DA assay demonstrated significant intracellular ROS elevation after treatment. JC-1 assay results showed a marked decrease in mitochondrial membrane potential ( $\Delta\Psi_m$ ), indicating mitochondrial outer membrane permeabilization. Apoptosis was confirmed by increased Annexin V/PI positivity and reduced cell viability in MTT assays.<sup>113</sup> Elias *et al.* (2024)<sup>114</sup> demonstrated novel Pt(II/IV) complexes which exhibit high anticancer potency (MTT assay) against both triple-negative breast cancer (MDA-MB-231) and cisplatin-resistant colorectal cancer (HT29). Mechanistic studies reveal: (A) substantial ROS induction (DCFH-DA assay); (B) mitochondrial membrane depolarization (JC-1 assay), consistent with MOMP; and (C) apoptotic and necrotic cell death (Annexin V-FITC/PI); primarily early apoptosis (Annexin V+/PI-), with some progression to late apoptosis/necrosis (Annexin V+/PI+).<sup>114</sup> Tabrizi *et al.* (2024)<sup>115</sup> synthesized platinum(IV) complexes designed to overcome cisplatin resistance in ovarian cancer. Mechanistic studies revealed: (A) ROS induction and GSH depletion (DCFH-DA and GSH assays), disrupting redox homeostasis; (B) mitochondrial dysfunction (JC-1 assay), showing decreased  $\Delta\Psi_m$  consistent with MOMP; and (C) DNA platination, indicating direct DNA binding and damage; and (D) apoptosis (Annexin V-FITC/PI), predominantly early apoptosis.<sup>115</sup>

Boodram *et al.* (2020)<sup>116</sup> synthesized a series of copper(II) complexes incorporating phenanthroline and indomethacin, with the most potent compound, complex **4**, demonstrating strong cytotoxicity against both CSC-enriched and CSC-depleted breast cancer cell populations as confirmed by MTT assay. Mechanistically, complex **4** exerts its anticancer effect through ROS-mediated DNA damage, as evidenced by plasmid DNA cleavage assays and redox activity studies showing hydrogen peroxide production *via* Cu(II)/Cu(I) cycling. The involvement of ROS was further validated by the use of scavengers (KI, Na<sub>2</sub>S<sub>2</sub>O<sub>3</sub>, *t*-BuOH, DMSO), which significantly reduced DNA damage, confirming oxidative stress as the primary driver. Apoptotic cell death was confirmed by western blot detection of caspase-3 activation and PARP cleavage, indicating activation of the intrinsic apoptotic pathway. Unlike classical DNA-alkylating agents, complex **4** does not rely on covalent DNA binding but induces cell death through oxidative DNA damage and subsequent caspase-dependent apoptosis, highlighting a mechanistic divergence from agents like cisplatin and placing it within the ROS induction and apoptosis-related categories.<sup>116</sup> Fei *et al.* (2019)<sup>117</sup> synthesized a series of chiral copper(II) complexes and evaluated their anticancer activity against MCF-7 breast cancer cells, uncovering a mechanism driven by oxidative stress and mitochondrial dysfunction. The complexes significantly depleted intracellular glutathione, thereby promoting the accumulation of reactive oxygen species, as measured by redox-sensitive assays. This increase in ROS led to oxidative DNA damage, confirmed by comet assay, which revealed characteristic DNA fragmentation. The DNA damage was followed by a marked decrease in mitochondrial membrane potential, as shown by JC-1 assay, indicating mitochondrial outer membrane permeabilization. This mitochondrial disruption initiated intrinsic apoptosis, as evi-

denced by the activation of caspase-9 and caspase-3, and further validated by Annexin V-FITC/PI staining. Collectively, these results establish that the copper(II) complexes induce apoptotic cell death through an ROS-dependent mechanism involving both DNA damage and mitochondrial collapse, placing their mode of action within ROS induction and mitochondrial disruption, with apoptosis as the downstream outcome.<sup>117</sup> Icel *et al.* (2020)<sup>118</sup> synthesized manganese(II) and copper(II) saccharinate complexes and assessed their anticancer potential in A549 lung cancer cells, identifying a mitochondria-mediated apoptotic mechanism. Both complexes exhibited strong cytotoxicity and showed concentration-dependent nuclease activity against supercoiled plasmid DNA, confirming their capacity for direct DNA interaction and cleavage. Mechanistic investigations revealed that complex treatment induced oxidative stress and caused mitochondrial membrane depolarization, as evidenced by JC-1 assay, leading to cytochrome c release into the cytosol. This mitochondrial dysfunction activated caspase-3 and caspase-7, confirming the initiation of intrinsic, caspase-dependent apoptosis. These findings place the mode of action of the Mn(II) and Cu(II) saccharinate complexes within DNA binding and cleavage, mitochondrial disruption, and apoptosis induction, with oxidative stress serving as a contributing factor to the cascade of cell death events.<sup>118</sup>

Hindo and colleagues synthesized and characterized three copper(II) coordination complexes with the iodo-substituted phenolic ligand HL<sup>+</sup>I: specifically [Cu(L<sup>+</sup>I)Cl] (**1**), [Cu(L<sup>+</sup>I)OAc] (**2**), and [Cu(HL<sup>+</sup>I)(L<sup>+</sup>I)]OAc (**3**). Each complex was designed to investigate the influence of metal-to-ligand stoichiometry (1 : 1 *vs.* 1 : 2) and ligand type on anticancer efficacy. Cytotoxicity assays revealed potent inhibitory effects against human prostate cancer cell lines C4-2B and PC-3, while sparing non-tumorigenic MCF-10A cells. Mechanistic assays demonstrated that these copper complexes selectively inhibit the chymotrypsin-like activity of the 20S proteasome, whereas the free ligand is inactive and copper salts showed only cell-free activity. This points to the copper-ligand coordination complex acting as the true pharmacophore. Proteasome inhibition was accompanied by accumulation of ubiquitinated proteins, consistent with disruption of protein degradation within cancer cells. Though not measured directly, the open coordination sphere likely enables binding nucleophilic residues (*e.g.* through the proteasome active site), enhancing specificity. No direct evidence was presented for ROS induction or mitochondrial disruption in this case. Instead, the primary mechanism is proteasome inhibition, with subsequent induction of apoptosis. These findings suggest that copper-ligand complexes can function as non-DNA-targeting, proteasome-inhibiting anticancer agents, offering a novel structural scaffold distinct from traditional genotoxic drugs.<sup>119</sup> Fei *et al.* (2021)<sup>120</sup> synthesized and characterized chiral copper(II) and iron(III) complexes derived from dehydroabiatic acid (DHA), a rosin-based natural product, to evaluate their structural and biological effects. The copper(II) complex (**1**) formed a dinuclear structure, while the iron(III) complex (**2**) was trinuclear. MTT assays

revealed that both complexes exhibited enhanced cytotoxicity compared with the free DHA ligand, with complex **1** showing superior activity against MCF-7 breast cancer cells. Mechanistic investigations demonstrated that both **1** and **2** induced oxidative stress, G<sub>1</sub> cell cycle arrest, and mitochondrial dysfunction, confirmed by mitochondrial membrane depolarization and decreased Bcl-2 expression. Apoptosis was triggered *via* both intrinsic (mitochondrial) and extrinsic (death receptor) pathways, evidenced by caspase-9 activation, Bax upregulation, and Fas/caspase-8/caspase-4 involvement, placing the complexes under death receptor activation and mitochondrial disruption. Notably, complex **1** also caused extensive damage to DNA, proteins, and lipids, and showed potential to inhibit cell migration, invasion, and angiogenesis, suggesting a multifaceted anticancer mechanism. Additionally, **1** was able to interact with Fas receptors on the cell surface, potentially initiating apoptosis without internalization. These findings establish complex **1** as a redox-active, multi-target anticancer agent combining ROS induction, dual-pathway apoptosis, and anti-metastatic properties.<sup>120</sup>

Li *et al.* (2019)<sup>121</sup> synthesized a series of ruthenium(II) polypyridyl complexes of the general formula Ru(bpy)<sub>2</sub>(L)<sub>2</sub>, where bpy is 2,2'-bipyridine and L is a substituted imidazo[4,5-*f*][1,10]phenanthroline derivative featuring a pendant amide or alkyl side chain to enhance biological activity and cellular uptake. Among these, the most active compound exhibited potent anticancer effects against HepG2 liver cancer cells. Mechanistic studies revealed that treatment with the ruthenium complex led to a marked loss of mitochondrial membrane potential ( $\Delta\Psi_m$ ), as measured by JC-1 assay, indicating mitochondrial dysfunction. This mitochondrial damage triggered downstream DNA fragmentation, confirmed by the comet assay, and ultimately led to apoptosis. Apoptotic cell death was supported by Annexin V-FITC/PI staining and caspase-3 activation, establishing a clear link between mitochondrial depolarization and programmed cell death. Overall, the results demonstrate that this ruthenium(II) complex exerts its anticancer activity *via* ROS-mediated mitochondrial disruption and secondary DNA damage, culminating in caspase-dependent apoptosis.<sup>121</sup> Chen *et al.* (2020)<sup>122</sup> developed a series of N-heterocyclic carbene (NHC)-coordinated ruthenium(II) arene complexes and assessed their anticancer activity, with Ru4 and Ru6 exhibiting the most potent cytotoxic effects against A2780 human ovarian cancer cells, as demonstrated by MTT assay. Mechanistic evaluation showed that both compounds significantly increased intracellular ROS levels, initiating oxidative stress. This oxidative environment led to mitochondrial dysfunction, evidenced by a marked loss of mitochondrial membrane potential ( $\Delta\Psi_m$ ), as detected by JC-1 staining. Western blot analysis revealed activation of caspase-9 and caspase-3, indicating the involvement of the intrinsic apoptotic pathway. Apoptosis induction was further supported by Annexin V-FITC/PI staining, which confirmed a substantial rise in apoptotic cell populations following treatment. These findings establish that Ru4 and Ru6 induce cancer cell death primarily through ROS-mediated mitochondrial disruption

(MoA4) and caspase-dependent apoptosis, positioning them as promising metal-based agents with a non-genotoxic but strongly apoptotic mechanism of action.<sup>122</sup> Chen *et al.* (2020)<sup>123</sup> synthesized two novel cyclometalated ruthenium(II) complexes, RuIQ-1 and RuIQ-2, bearing isoquinoline-based ligands coordinated through both nitrogen and carbon donor atoms. These half-sandwich Ru(II) complexes feature the general motif  $[(\eta^6\text{-}p\text{-cymene})\text{Ru}(\text{C}^{\wedge}\text{N})(\text{L})]^+$ , where C<sup>^</sup>N represents the cyclometalated isoquinoline ligand and L is a neutral co-ligand, designed to enhance both redox activity and lipophilicity for improved anticancer efficacy. Both RuIQ-1 and RuIQ-2 exhibited strong cytotoxicity against NCI-H460 human non-small cell lung cancer cells, as demonstrated by MTT assay. Mechanistic studies revealed that treatment with either complex resulted in significant overproduction of intracellular reactive oxygen species (ROS), as measured by DCFH-DA assay, alongside marked mitochondrial membrane depolarization, confirmed *via* JC-1 staining. This oxidative stress and mitochondrial dysfunction triggered caspase-9 and caspase-3 activation, verified by western blotting, establishing the activation of the intrinsic apoptotic pathway. DNA damage was further validated using the comet assay, which showed extensive strand breaks following treatment. Apoptosis was confirmed as the mode of cell death by Annexin V-FITC/PI double staining, which indicated a substantial increase in apoptotic cell populations. Taken together, these results confirm that RuIQ-1 and RuIQ-2 induce caspase-dependent apoptosis through a mechanism driven by ROS generation, mitochondrial disruption, and oxidative DNA damage, representing a multifaceted and redox-driven mode of action distinguished from DNA-alkylating agents like cisplatin.<sup>123</sup> Allison *et al.* (2023)<sup>124</sup> synthesized and characterized a library of 24 cyclometalated ruthenium(II) arene complexes of the type  $[(p\text{-cymene})\text{RuCl}(\text{Fc-acac})]$ , incorporating functionalized ferrocenyl  $\beta$ -diketonate ligands (Fc-acac). Structural confirmation was obtained for 21 of the compounds *via* single-crystal X-ray diffraction. These complexes were screened for cytotoxicity against MIA PaCa-2 pancreatic cancer cells, HCT116 p53+/+ colorectal cancer cells, and ARPE-19 normal retinal cells. Complex **4** (R = 2-furan) emerged as the most potent and selective candidate, showing an IC<sub>50</sub> of  $8 \pm 2$   $\mu\text{M}$  against MIA PaCa-2 cells and a selectivity index (SI) of 12.5, as determined by MTT assay. Mechanistic studies revealed that complex **4** induced significant DNA damage in a dose-dependent manner, confirmed by single-strand break (SSB) detection in MIA PaCa-2 cells, suggesting direct genotoxicity as a primary cytotoxic mechanism. Although cyclic voltammetry indicated a reversible Fc/Fc<sup>+</sup> redox couple, and the structure suggested ROS-generating potential, no direct functional assays (*e.g.*, DCFH-DA or GSH depletion) were performed to confirm ROS involvement. UV-vis and NMR studies indicated gradual degradation of the Ru–Cl bond and ligand dissociation, which may influence biological stability and uptake, partially explaining the discrepancy between intracellular ruthenium levels and cytotoxic efficacy (*via* ICP-MS). Under hypoxic conditions (0.1% O<sub>2</sub>), cytotoxicity decreased, mirroring cisplatin's behavior and suggesting that redox activity may still

play a supporting role. Overall, complex **4** exerts its anticancer effects primarily through DNA strand damage, with a potential but unconfirmed contribution of oxidative stress, making it a promising non-platinum redox-active scaffold with selective anticancer properties.<sup>124</sup> Pettinari *et al.* (2014)<sup>125</sup> synthesized a series of nine novel arene–ruthenium(II) complexes incorporating 4-(biphenyl-4-carbonyl)-3-methyl-1-phenyl-5-pyrazolonate as the chelating ligand, with structural variations in the arene moiety (notably including hexamethylbenzene) aimed at modulating biological activity. These complexes were structurally characterized *via* spectroscopic techniques and X-ray diffraction. Cytotoxicity screening against HeLa, MCF-7, HepG2, and HCT116 human cancer cell lines revealed that compounds **3**, **6**, and **9**—those containing hexamethylbenzene as the arene—exhibited the most potent cytotoxicity, with IC<sub>50</sub> values comparable to cisplatin. Mechanistic studies demonstrated that these compounds induce caspase-dependent apoptosis, as confirmed by increased DEVDase (caspase-3/7-like) activity, enhanced DNA fragmentation, upregulation of pro-apoptotic proteins, and downregulation of the anti-apoptotic protein Bcl-2. Additionally, flow cytometry showed G<sub>2</sub>/M cell cycle arrest, likely due to DNA interaction. Competitive binding and intercalation assays confirmed that compounds **1**, **3**, **4**, and **6** selectively bind to the minor groove of dsDNA and are capable of intercalating DNA, indicating direct DNA interaction and damage as a contributing factor to cytotoxicity. These findings support a dual mechanism of action involving both DNA binding and mitochondria-mediated apoptosis, modulated by the nature of the arene and ancillary ligands, and provide a rational basis for further structural optimization of ruthenium-based anticancer agents.<sup>125</sup>

Truong *et al.* (2020)<sup>126</sup> synthesized a series of Rh(III) and Ir(III) half-sandwich complexes of the general formula [M(Cp\*) (NHC)Cl<sub>2</sub>], where Cp\* is pentamethylcyclopentadienyl and NHC represents a benzyl- or methyl-substituted N-heterocyclic carbene ligand. These complexes were designed as analogues to previously reported Ru(II) and Os(II) systems, aiming to explore how changes in the metal center and ligand structure affect biological activity. The Rh(III) complexes, particularly **3a** and **3b**, demonstrated potent inhibition of thioredoxin reductase (TrxR) with IC<sub>50</sub> values around 1 μM, as validated by enzyme inhibition assays. Despite their strong TrxR inhibitory activity, complex **3a** showed limited cytotoxicity, likely due to lower lipophilicity and reduced cellular uptake, while **3b** exhibited significantly better antiproliferative potency, highlighting the role of hydrophobic ligand substitution in enhancing biological effects. Importantly, X-ray fluorescence microscopy (XFM) confirmed cytoplasmic accumulation of the Ru and Os analogues, with minimal nuclear localization, supporting a non-DNA-targeting mechanism of action. These findings establish that the cytotoxic activity of Rh(III) complexes is primarily mediated through TrxR inhibition rather than DNA interaction, and that structural modulation of NHC substituents can significantly influence both enzyme inhibition and cellular uptake.<sup>126</sup>

Atrián-Blasco *et al.* (2017)<sup>127</sup> synthesized a series of novel gold(I) thiolate derivatives stabilized by water-soluble phosphane ligands derived from 1,3,5-triaza-7-phosphaadamantane

(PTA), forming oligomeric [ $\{\text{Au}(\text{thiolate})\}_n$ ] species. These complexes were designed to enhance chemical stability and anticancer efficacy over previously studied halide-containing analogues. Cytotoxicity screening against human colon cancer cell lines revealed potent antiproliferative activity, with significantly higher chemical stability in buffered aqueous environments contributing to their enhanced biological performance. Mechanistic studies indicated that these gold(I) thiolate complexes induce apoptotic cell death, supported by elevated intracellular ROS levels, likely resulting from inhibition of thioredoxin reductase (TrxR), thereby disrupting the redox homeostasis within cancer cells. While direct DNA interaction was not observed, the redox imbalance induced by TrxR inhibition plays a central role in the cytotoxic mechanism. Importantly, these compounds demonstrated selective cytotoxicity, sparing normal enterocyte Caco-2 cells under confluence, and exhibited synergistic effects with 5-fluorouracil (5-FU), reducing the effective dose of 5-FU by up to 40-fold when used in combination. Overall, these findings establish that the gold(I) thiolate complexes exert their anticancer effects primarily *via* ROS-mediated apoptosis triggered by TrxR inhibition and hold promise as selective adjuvants in combination chemotherapy for colon cancer.<sup>127</sup> Mármol *et al.* (2017)<sup>128</sup> investigated the anticancer activity of a novel alkynyl gold(I) complex, [Au(C≡C-2-NC<sub>5</sub>H<sub>4</sub>)(PTA)], featuring a pyridylacetylidate ligand and 1,3,5-triaza-7-phosphaadamantane (PTA) as the phosphine donor. The complex demonstrated significant cytotoxicity against Caco-2 colorectal adenocarcinoma cells, as confirmed by MTT assay. Mechanistic studies revealed a marked increase in intracellular reactive oxygen species (ROS), detected *via* DCFH-DA assay, which led to a disruption of mitochondrial membrane potential ( $\Delta\Psi_m$ ), as shown by JC-1 staining. While Annexin V-FITC/PI staining indicated some apoptotic membrane changes, caspase-3/7 activity remained minimal, and a comet assay confirmed the absence of DNA damage, ruling out apoptosis and genotoxicity as primary pathways. Importantly, necroptosis-specific inhibition assays demonstrated that the predominant mode of cell death was necroptosis, a regulated necrotic pathway driven by oxidative stress and mitochondrial dysfunction. These findings establish that the alkynyl gold(I) complex induces cell death through an ROS-mediated, non-apoptotic mechanism centered on mitochondrial impairment and caspase-independent necroptosis, distinguishing it mechanistically from both traditional apoptotic inducers and DNA-targeting metal drugs.<sup>128</sup> Quero *et al.* (2022)<sup>129</sup> synthesized a series of sulfonamide-derived dithiocarbamate gold(I) complexes and assessed their anticancer properties against Caco-2 colon cancer cells. Among the compounds evaluated, [Au(S<sub>2</sub>CNHSO<sub>2</sub>C<sub>6</sub>H<sub>5</sub>)(PPh<sub>3</sub>)] (**1**) and [Au(S<sub>2</sub>CNHSO<sub>2</sub>-*p*-Me-C<sub>6</sub>H<sub>4</sub>)(IMePropargyl)] (**8**) exhibited the most potent cytotoxic activity, as determined by MTT assay. Mechanistic investigations revealed that both complexes significantly increased intracellular reactive oxygen species (ROS), as measured by DCFH-DA assay, and disrupted mitochondrial membrane potential ( $\Delta\Psi_m$ ), confirmed by JC-1 staining. Western blot analysis showed activation of caspase-3, and

Annexin V-FITC/PI staining further confirmed the induction of apoptosis over necrosis. Additionally, both complexes were shown to inhibit thioredoxin reductase (TrxR), suggesting a redox-mediated mechanism. These findings support a mode of action driven by TrxR inhibition and ROS-mediated mitochondrial dysfunction, culminating in caspase-dependent intrinsic apoptosis. The lack of necrotic or DNA-targeting effects highlights a redox-regulated apoptotic pathway distinct from genotoxic chemotherapeutics.<sup>129</sup> In a study by Gutiérrez *et al.*, gold(i) thiolate complexes were designed to incorporate amino acid-derived ligands (notably complexes **6** and **21**) to evaluate their cytotoxicity and elucidate their mechanisms of cell death against human cancer cell lines A549 (lung carcinoma) and Jurkat (T-cell leukemia). Mechanistic studies revealed that the mode of cell death induced by these gold(i) complexes varied between cell lines. In A549 cells, no typical apoptotic nuclear morphology (chromatin condensation or fragmentation) was observed, indicating non-apoptotic cell death, whereas in Jurkat cells, both apoptosis and necrosis contributed to cell death. Flow cytometry using Annexin V-PE and 7-AAD staining supported these observations, showing phosphatidylserine externalization typical of apoptosis alongside loss of membrane integrity indicative of necrosis. The role of oxidative stress was confirmed as antioxidants *N*-acetyl cysteine (NAC) and glutathione (GSH) protected cells from the cytotoxic effects, though the protection profile differed between cell types, suggesting cell-dependent mechanisms. Further investigations showed that both complexes induced a significant decrease in mitochondrial membrane potential (MMP), with a stronger effect in Jurkat cells. The mitochondrial dysfunction was closely correlated with increased intracellular reactive oxygen species (ROS) production, particularly marked with complex **21**. These data suggest that mitochondrial damage leads to ROS overproduction, which contributes to cell death. Additionally, both complexes potently inhibited thioredoxin reductase (TrxR) activity (~50% inhibition by complex **6** and ~65% by complex **21** near IC<sub>50</sub> concentrations), an enzyme crucial for maintaining cellular redox balance. This inhibition likely prevents ROS detoxification, promoting oxidative stress and contributing to cytotoxicity. In conclusion, these gold(i) amino acid thiolate complexes induce cell death through mechanisms involving mitochondrial dysfunction, ROS overproduction, and TrxR inhibition, with a combined apoptosis and necrosis phenotype that varies by cell line. These results highlight the importance of redox balance disruption in their anticancer activity.<sup>130</sup>

Yanci Li *et al.* synthesized and characterized a series of palladium(II) complexes of curcuminoids, focusing on complex **3h** for its potent anticancer activity. The MTT assay revealed strong cytotoxicity of complex **3h** against various cancer cell lines. Mechanistic studies demonstrated that treatment with **3h** led to significant overproduction of reactive oxygen species (ROS), confirmed by ROS assays. The addition of the antioxidant *N*-acetyl cysteine (NAC) effectively reduced both ROS levels and cell death, validating an ROS-dependent mechanism. Further analysis using Annexin V-FITC/PI staining and

Hoechst nuclear staining indicated clear apoptotic features in treated cells. A marked loss of mitochondrial membrane potential was detected, signifying mitochondrial dysfunction. Additionally, cell cycle assays showed that complex **3h** induced cell cycle arrest in the S phase. Together, these results confirm that palladium(II) complex **3h** induces apoptosis *via* an ROS-mediated mitochondrial pathway, highlighting the role of oxidative stress and mitochondrial impairment in its antitumor effect.<sup>131</sup> Kazem Karami *et al.* synthesized two novel palladium(II)-hydrazide complexes and evaluated their anticancer potential. Plasmid DNA cleavage assays revealed that these complexes induce oxidative DNA damage, identifying DNA as a primary molecular target. Complementary DNA binding studies indicated likely intercalative interaction with DNA. This DNA damage was shown to be the key trigger for cell death. Annexin V-FITC/PI staining of CT26 cells confirmed that the complexes induce apoptosis as the dominant mode of cell death, with over 93% of treated cells undergoing programmed cell death. Together, these findings establish that the palladium complexes exert cytotoxicity through DNA damage-induced apoptosis.<sup>132</sup>

## 6 Conclusion

This review underscores the critical role of well-designed biochemical assays in advancing the development of metal-based anticancer drugs. Metal-based coordination and organometallic compounds represent a rapidly evolving class of chemotherapeutic agents with diverse mechanisms of action, ranging from classical DNA damage to redox modulation, proteasome inhibition, and mitochondrial disruption. The success of platinum-based drugs has inspired the exploration of other transition metals (*e.g.*, Ru, Au, Cu, Pd), whose unique chemical properties enable targeted interactions with biomolecules critical for cancer cell survival. However, the development of these agents is often hindered by mechanistic over-interpretation and insufficient validation, emphasizing the need for rigorous experimental strategies.

We highlight three key considerations for future research:

(A) Multi-assay validation is essential: reliance on a single endpoint (*e.g.*, MTT for cytotoxicity) is inadequate; complementary techniques—such as Annexin V/PI staining, JC-1 mitochondrial assays, TrxR inhibition assays, and emerging proteomic tools—are necessary to confirm mechanisms with confidence.

(B) Structural similarity does not guarantee mechanistic similarity: even minor modifications in ligand frameworks, as seen with Pt(II) terpyridine *versus* ferrocenyl complexes, can shift activity from DNA binding to ROS-mediated apoptosis or lysosomal disruption. Likewise, Cu(II) complexes exhibit mechanistic diversity, ranging from oxidative DNA damage to proteasome inhibition and death receptor activation.

(C) Emerging non-apoptotic pathways hold promise: strategies targeting redox homeostasis (*e.g.*, TrxR inhibition by Au(I/III) complexes), proteasome function (*e.g.*, Cu(II) complexes),

and regulated necrosis (e.g., ferroptosis, necroptosis) offer alternatives to overcome cisplatin resistance and toxicity associated with classical apoptosis.

By integrating traditional cytotoxicity and apoptosis assays with cutting-edge label-free methods such as CETSA and TPP, researchers can accurately outline polypharmacological effects and engage alternative cell death pathways. The future of metal-based drugs lies in rational design guided by robust, multi-assay mechanistic data. This integrated approach will minimize overinterpretation and accelerate the development of selective, multitargeted agents capable of overcoming therapeutic resistance and improving clinical outcomes.

## Conflicts of interest

There are no conflicts to declare.

## Data availability

This article is a review and does not report any new data. All data discussed are derived from previously published studies, which are appropriately cited throughout the manuscript. No new datasets were generated or analyzed during the preparation of this work.

## References

- World Health Organization. Global Cancer Burden Growing, Amidst Mounting Need for Services. 1 Feb. 2024, <https://www.who.int/news/item/01-02-2024-global-cancer-burden-growing-amidst-mounting-need-for-services>.
- C. Zhang, C. Xu, X. Gao and Q. Yao, Platinum-based drugs for cancer therapy and anti-tumor strategies, *Theranostics*, 2022, **12**(5), 2115–2132.
- J. J. Wilson and S. J. Lippard, Synthetic Methods for the Preparation of Platinum Anticancer Complexes, *Chem. Rev.*, 2014, **114**(8), 4470–4495.
- X. Lia, A. Gorlea, M. Sundaraneedia, R. Keeneb and J. G. Collins, Kinetically-inert polypyridyl ruthenium(II) complexes as therapeutic agents, *Coord. Chem. Rev.*, 2018, **375**, 134–147.
- S. Y. Lee, C. Y. Kim and T. G. Nam, Ruthenium Complexes as Anticancer Agents: A Brief History and Perspectives, *Drug Des., Dev. Ther.*, 2020, **14**, 5375–5392.
- J. R. Stenger-Smith and P. K. Mascharak, Gold Drugs with {Au(PPh<sub>3</sub>)<sub>3</sub>}<sup>+</sup> moiety: Advantages and Medicinal Applications, *ChemMedChem*, 2020, **15**, 2136–2145.
- T. Zou, C. T. Lum, C.-N. Lok, J.-J. Zhang and C.-M. Che, Chemical biology of anticancer gold(III) and gold(I) complexes, *Chem. Soc. Rev.*, 2015, **44**, 8786–8801.
- X. Tang, Z. Yan, Y. Miao, W. Ha, Z. Li, L. Yang and D. Mi, Copper in cancer: from limiting nutrient to therapeutic target, *Front. Oncol.*, 2023, **13**, 1209156.
- S. Abdolmaleki, A. Aliabadi and S. Khaksar, Unveiling the promising anticancer effect of copper based compounds: a comprehensive review, *J. Cancer Res. Clin. Oncol.*, 2024, 150–213.
- A. R. Kapdi and I. J. S. Fairlamb, Anti-cancer palladium complexes: a focus on PdX<sub>2</sub>L<sub>2</sub>, palladacycles and related complexes, *Chem. Soc. Rev.*, 2014, **43**, 4751–4777.
- F. Trudua, F. Amato, P. Vañhara, T. Pivetta, E. M. Peña-Méndez and J. Havel, Coordination compounds in cancer: Past, present and perspectives, *J. Appl. Biomed.*, 2015, **13**, 79–103.
- A. M. Pizarro, A. Habtemariam and P. J. Sadler, Activation Mechanisms for Organometallic Anticancer Complexes, *Top. Organomet. Chem.*, 2010, **32**, 21–56.
- T. Mosmann, Rapid colorimetric assay for cellular growth and survival: Application to proliferation and cytotoxicity assays, *J. Immunol. Methods*, 1983, **65**, 55–63.
- P. W. Sylvester, Analysis of the MTT Assay: Protocols and Interpretation, *Methods Mol. Biol.*, 2011, **716**, 157–168.
- J. C. Stockert, R. W. Horobin, L. L. Colombo and A. Blázquez-Castro, Tetrazolium salts and formazan products in Cell Biology: Viability assessment, fluorescence imaging, and labeling perspectives, *Acta Histochem.*, 2018, **120**(3), 159–167.
- P. Skehan, R. Storeng, D. Scudiero, A. Monks, J. McMahon, D. Vistica, J. T. Warren, H. Bokesch, S. Kenney and M. R. Boyd, New Colorimetric Cytotoxicity Assay for Anticancer-Drug Screening, *J. Natl. Cancer Inst.*, 1990, **82**(13), 1107–1112.
- V. Vichai and K. Kirtikara, Sulforhodamine B colorimetric assay for cytotoxicity screening, *Nat. Protoc.*, 2006, **1**, 1112–1116.
- K. T. Papazisis, G. D. Geromichalos, K. A. Dimitriadis and A. H. Kortsaris, Optimization of the sulforhodamine B colorimetric assay, *J. Immunol. Methods*, 1997, **208**(2), 151–158.
- H. Krämer, M. Amouyal, A. Nordheim and B. Müller-Hill, DNA supercoiling changes the spacing requirement of two lac operators for DNA loop formation with lac repressor, *EMBO J.*, 1988, **7**(2), 547–556.
- C. Guthrie and G. R. Fink, Plasmid DNA cleavage assays for nucleases and DNA-damaging agents. In: Guide to yeast genetics and molecular biology, *Methods Enzymol.*, 1991, **194**, 481–490.
- N. P. Singh, M. T. McCoy, R. R. Tice and E. L. Schneider, A simple technique for quantitation of low levels of DNA damage in individual cells, *Exp. Cell Res.*, 1988, **175**(1), 184–191.
- R. R. Tice, E. Agurell, D. Anderson, B. Burlinson, A. Hartmann, H. Kobayashi, Y. Miyamae, E. Rojas, J. C. Ryu and Y. F. Sasaki, Single cell gel/comet assay: guidelines for in vitro and in vivo genetic toxicology testing, *Environ. Mol. Mutagen.*, 2000, **35**(3), 206–221.
- N. Jiang, S. Naz, Y. Ma, Q. Ullah, M. Z. Khan, J. Wang, X. Lu, D.-Z. Luosang, S. Tabassum, A. M. M. Chatha and W.-D. Basang, An Overview of Comet Assay Application for

- Detecting DNA Damage in Aquatic Animals, *Agriculture*, 2023, **13**, 623.
- 24 A. R. Collins, The comet assay for DNA damage and repair: principles, applications, and limitations, *Mol. Biotechnol.*, 2004, **26**(3), 249–261.
- 25 J. Marmur and P. Doty, Determination of the base composition of deoxyribonucleic acid from its thermal denaturation temperature, *J. Mol. Biol.*, 1962, **5**, 109–118.
- 26 C. T. Wittwer, A. C. Hemmert, J. O. Kent and N. A. Rejali, DNA melting analysis, *Mol. Aspects Med.*, 2024, **97**, 101268.
- 27 J. B. Chaires, Calorimetry and thermodynamics in drug design, *Annu. Rev. Biophys.*, 2008, **37**, 135–151.
- 28 G. Koopman, C. P. Reutelingsperger, G. A. Kuijten, R. M. Keehnen, S. T. Pals and M. H. van Oers, Annexin V for flow cytometric detection of phosphatidylserine expression on B cells undergoing apoptosis, *Blood*, 1994, **84**(5), 1415–1420.
- 29 I. Vermes, C. Haanen, H. Steffens-Nakken and C. Reutelingsperger, A novel assay for apoptosis: Flow cytometric detection of phosphatidylserine expression on early apoptotic cells using fluorescein labelled Annexin V, *J. Immunol. Methods*, 1995, **184**(1), 39–51.
- 30 J. Yuan, S. Shaham, S. Ledoux, H. M. Ellis and H. R. Horvitz, The *C. elegans* cell death gene *ced-3* encodes a protein similar to mammalian interleukin-1 beta-converting enzyme, *Cell*, 1993, **75**(4), 641–652.
- 31 D. W. Nicholson, A. Ali, N. A. Thornberry, J. P. Vaillancourt, C. K. Ding, M. Gallant, Y. Gareau, P. R. Griffin, M. Labelle, Y. A. Lazebnik, N. A. Munday, S. M. Raju, M. E. Smulson, T.-T. Yamin, V. L. Yu and D. K. Miller, Identification and inhibition of the ICE/CED-3 protease necessary for mammalian apoptosis, *Nature*, 1995, **376**(6535), 37–43.
- 32 N. A. Thornberry, T. A. Rano, E. P. Peterson, D. M. Rasper, T. Timkey, M. Garcia-Calvo, V. M. Houtzager, P. A. Nordstrom, S. Roy, J. P. Vaillancourt, K. T. Chapman and D. W. Nicholson, A combinatorial approach defines specificities of members of the caspase family and granzyme B. Functional relationships established for key mediators of apoptosis, *J. Biol. Chem.*, 1997, **272**(29), 17907–17911.
- 33 C. Pop, G. S. Salvesen and F. L. Scott, Caspase assays: identifying caspase activity and substrates in vitro and in vivo, *Methods Enzymol.*, 2008, **446**, 351–367.
- 34 D. R. McIlwain, T. Berger and T. W. Mak, Caspase functions in cell death and disease, *Cold Spring Harbor Perspect. Biol.*, 2013, **5**(4), a008656.
- 35 L. Galluzzi, S. A. Aaronson, J. Abrams, E. S. Alnemri, D. W. Andrews, E. H. Baehrecke, N. G. Bazan, M. V. Blagosklonny, K. Blomgren, C. Borner, D. E. Bredesen, C. Brenner, M. Castedo, J. A. Cidlowski, A. Ciechanover, G. M. Cohen, V. De Laurenzi, R. De Maria, M. Deshmukh, B. D. Dynlacht, W. S. El-Deiry, R. A. Flavell, S. Fulda, C. Garrido, P. Golstein, M. L. Gougeon, D. R. Green, H. Gronemeyer, G. Hajnóczky, J. M. Hardwick, M. O. Hengartner, H. Ichijo, M. Jäättelä, O. Kepp, A. Kimchi, D. J. Klionsky, R. A. Knight, S. Kornbluth, S. Kumar, B. Levine, S. A. Lipton, E. Lugli, F. Madeo, W. Malomi, J. C. Marine, S. J. Martin, J. P. Medema, P. Mehlen, G. Melino, U. M. Moll, E. Morselli, S. Nagata, D. W. Nicholson, P. Nicotera, G. Nuñez, M. Oren, J. Penninger, S. Pervaiz, M. E. Peter, M. Piacentini, J. H. Prehn, H. Puthalakath, G. A. Rabinovich, R. Rizzuto, C. M. Rodrigues, D. C. Rubinsztein, T. Rudel, L. Scorrano, H. U. Simon, H. Steller, J. Tschopp, Y. Tsujimoto, P. Vandenabeele, I. Vitale, K. H. Vousden, R. J. Youle, J. Yuan, B. Zhivotovsky and G. Kroemer, Guidelines for the use and interpretation of assays for monitoring cell death in higher eukaryotes, *Cell Death Differ.*, 2009, **16**(8), 1093–1107.
- 36 S. T. Smiley, M. Reers, C. Mottola-Hartshorn, M. Lin, A. Chen, T. W. Smith, G. D. Steele Jr and L. B. Chen, Intracellular heterogeneity in mitochondrial membrane potentials revealed by a J-aggregate-forming lipophilic cation JC-1, *Proc. Natl. Acad. Sci. U. S. A.*, 1991, **88**(9), 3671–3675.
- 37 A. Cossarizza, C. M. Baccarani, G. Kalashnikova and C. Franceschi, A new method for the cytofluorimetric analysis of mitochondrial membrane potential using the J-aggregate forming lipophilic cation 5,5',6,6'-tetrachloro-1,1',3,3'-tetraethylbenzimidazolcarbocyanine iodide (JC-1), *Biochem. Biophys. Res. Commun.*, 1993, **197**, 40–45.
- 38 K. Elefantova, B. Lakatos, J. Kubickova, Z. Sulova and A. Breier, Detection of the Mitochondrial Membrane Potential by the Cationic Dye JC-1 in L1210 Cells with Massive Overexpression of the Plasma Membrane ABCB1 Drug Transporter, *Int. J. Mol. Sci.*, 2018, **19**, 1985.
- 39 C. Pal, Mitochondria-targeted metallo-drugs against cancer: A current mechanistic perspective, *Results Chem.*, 2023, **6**, 101149.
- 40 P. Marchetti, M. Castedo, S. A. Susin, N. Zamzami, T. Hirsch, A. Macho, A. Haeflner, F. Hirsch, M. Geuskens and G. Kroemer, Mitochondrial permeability transition is a central coordinating event of apoptosis, *J. Exp. Med.*, 1996, **184**(3), 1155–1160.
- 41 S. W. Perry, J. P. Norman, J. Barbieri, E. B. Brown and H. A. Gelbard, Mitochondrial membrane potential probes and the proton gradient: a practical usage guide, *BioTechniques*, 2011, **50**(2), 98–115.
- 42 A. S. Keston and R. Brandt, The fluorometric analysis of ultramicro quantities of hydrogen peroxide, *Anal. Biochem.*, 1965, **11**, 1–5.
- 43 C. P. LeBel, H. Ischiropoulos and S. C. Bondy, Evaluation of the Probe 2',7'-Dichlorofluorescein as an Indicator of Reactive Oxygen Species Formation and Oxidative Stress, *Chem. Res. Toxicol.*, 1992, **5**, 227–231.
- 44 H. Kim and X. Xue, Detection of Total Reactive Oxygen Species in Adherent Cells by 2',7'-Dichlorodihydrofluorescein Diacetate Staining, *J. Visualized Exp.*, 2020, **160**, DOI: [10.3791/60682](https://doi.org/10.3791/60682).

- 45 B. Kalyanaraman, V. Darley-USmar, K. J. Davies, P. A. Dennery, H. J. Forman, M. B. Grisham, G. E. Mann, K. Moore, L. J. Roberts and H. Ischiropoulos, Measuring reactive oxygen and nitrogen species with fluorescent probes: challenges and limitations, *Free Radicals Biol. Med.*, 2012, **52**(1), 1–6.
- 46 F. Tietze, Enzymic method for quantitative determination of nanogram amounts of total and oxidized glutathione: Applications to mammalian blood and other tissues, *Anal. Biochem.*, 1969, **27**(3), 502–522.
- 47 V. Ribas, C. García-Ruiz and J. C. Fernández-Checa, Glutathione and mitochondria, *Front. Pharmacol.*, 2014, **5**, 151.
- 48 O. W. Griffith, Determination of glutathione and glutathione disulfide using glutathione reductase and 2-vinylpyridine, *Anal. Biochem.*, 1980, **106**(1), 207–212.
- 49 D. Giustarini, I. Dalle-Donne, A. Milzani, P. Fanti and R. Rossi, Analysis of GSH and GSSG after derivatization with N-ethylmaleimide, *Nat. Protoc.*, 2013, **8**, 1660–1669.
- 50 J. Nordberg, L. Zhong, A. Holmgren and E. S. Arner, Mammalian thioredoxin reductase is irreversibly inhibited by dinitrohalobenzenes by alkylation of both the redox active selenocysteine and its neighboring cysteine residue, *J. Biol. Chem.*, 1998, **273**, 10835–10842.
- 51 E. S. Arnér and A. Holmgren, Physiological functions of thioredoxin and thioredoxin reductase, *Eur. J. Biochem.*, 2000, **267**(20), 6102–6109.
- 52 E. S. Arnér, Focus on mammalian thioredoxin reductases—important selenoproteins with versatile functions, *Biochim. Biophys. Acta*, 2009, **1790**(6), 495–526.
- 53 M. Orlowski and S. Wilk, A multicatalytic protease complex from pituitary that forms enkephalin and enkephalin containing peptides, *Biochem. Biophys. Res. Commun.*, 1981, **101**(3), 814–822.
- 54 A. F. Kisselev and A. L. Goldberg, Monitoring activity and inhibition of 26S proteasomes with fluorogenic peptide substrates, *Methods Enzymol.*, 2005, **398**, 364–378.
- 55 J. Adams, V. J. Palombella, E. A. Sausville, J. Johnson, A. Destree, D. D. Lazarus, J. Maas, C. S. Pien, S. Prakash and P. J. Elliott, Proteasome Inhibitors: A Novel Class of Potent and Effective Antitumor Agents, *Cancer Res.*, 1999, **59**(11), 2615–2622.
- 56 J. Adams, The proteasome: Structure, function, and role in the cell, *Cancer Treat. Rev.*, 2003, **30**(1), 1–9.
- 57 A. Ciechanover, Proteolysis: From the lysosome to ubiquitin and the proteasome, *Nat. Rev. Mol. Cell Biol.*, 2005, **6**(1), 79–87.
- 58 M. Mishra, S. Tiwari and A. V. Gomes, Protein purification and analysis: next generation Western blotting techniques, *Expert Rev. Proteomics*, 2017, **14**(11), 1037–1053.
- 59 S. T. Nawrocki, J. S. Carew, K. Dunner Jr., L. H. Boise, P. J. Chiao, P. Huang, J. L. Abbruzzese and D. J. McConkey, Bortezomib inhibits PKR-like endoplasmic reticulum (ER) kinase and induces apoptosis via ER stress in human pancreatic cancer cells, *Cancer Res.*, 2005, **65**(24), 11510–11519.
- 60 Z. Darzynkiewicz, G. Juan and E. Bedner, Determining cell cycle stages by flow cytometry, in *Curr. Protoc. Cell Biol.*, 2001, DOI: [10.1002/0471143030.cb0804s01](https://doi.org/10.1002/0471143030.cb0804s01).
- 61 P. Pozarowski and Z. Darzynkiewicz, Analysis of cell cycle by flow cytometry, *Methods Mol. Biol.*, 2004, **281**, 301–311.
- 62 C. Riccardi and I. Nicoletti, Analysis of apoptosis by propidium iodide staining and flow cytometry, *Nat. Protoc.*, 2006, **1**, 1458–1461.
- 63 T. E. Angel, U. K. Aryal, S. M. Hengel, E. S. Baker, R. T. Kelly, E. W. Robinson and R. D. Smith, Mass spectrometry-based proteomics: existing capabilities and future directions, *Chem. Soc. Rev.*, 2012, **41**(10), 3912–3928.
- 64 D. Martinez Molina, R. Jafari, M. Ignatushchenko, T. Seki, E. A. Larsson, C. Dan, L. Sreekumar, Y. Cao and P. Nordlund, Monitoring drug target engagement in cells and tissues using the cellular thermal shift assay, *Science*, 2013, **341**(6141), 84–87.
- 65 D. Martinez Molina and P. Nordlund, The Cellular Thermal Shift Assay: A Novel Biophysical Assay for In Situ Drug Target Engagement and Mechanistic Biomarker Studies, *Annu. Rev. Pharmacol. Toxicol.*, 2016, **56**, 141–161.
- 66 M. M. Savitski, F. B. Reinhard, H. Franken, T. Werner, M. F. Savitski, D. Eberhard, D. M. Molina, R. Jafari, R. B. Dovega, S. Klaeger, B. Kuster, P. Nordlund, M. Bantscheff and G. Drewes, Tracking cancer drugs in living cells by thermal profiling of the proteome, *Science*, 2014, **346**(6205), 1255784.
- 67 C. Le Sueur, H. M. Hammarén, S. Sridharan and M. M. Savitski, Thermal proteome profiling: Insights into protein modifications, associations, and functions, *Curr. Opin. Chem. Biol.*, 2022, **71**, 102225.
- 68 J. Moffat, J. Rudolph and D. Bailey, Phenotypic screening in cancer drug discovery—past, present and future, *Nat. Rev. Drug Discovery*, 2014, **13**, 588–602.
- 69 M. Winiewska-Szajewska and J. Poznański, Differential scanning fluorimetry followed by microscale thermophoresis and/or isothermal titration calorimetry as an efficient tool for ligand screening, *Biophys. Rev.*, 2025, **17**, 199–223.
- 70 V. Upadhyay, A. Lucas, C. Patrick and K. M. G. Mallela, Isothermal titration calorimetry and surface plasmon resonance methods to probe protein-protein interactions, *Methods*, 2024, **225**, 52–61.
- 71 F. Soltermann, W. B. Struwe and P. Kukura, Label-free methods for optical *in vitro* characterization of protein-protein interactions, *Phys. Chem. Chem. Phys.*, 2021, **23**(31), 16488–16500.
- 72 X. Wang, P. Hua, C. He and M. Chen, Non-apoptotic cell death-based cancer therapy: Molecular mechanism, pharmacological modulators, and nanomedicine, *Acta Pharm. Sin. B*, 2022, **12**(9), 3567–3593.
- 73 J. Gonçalves, J. D. Amaral, R. Capela, M. J. Perry, C. Braga, M. M. Gaspar, F. M. Piedade, L. Bijlsma, A. Roig, S. N. Pinto, R. Moreira, P. Florindo and C. M. P. Rodrigues, Necroptosis induced by ruthenium(II) complexes as mitochondrial disruptors, *Cell Death Discovery*, 2024, **10**, 261.

- 74 K. Xiong, C. Qian, Y. Yuan, L. Wei, X. Liao, L. He, T. W. Rees, Y. Chen, J. Wan, L. Ji and H. Chao, Necroptosis Induced by Ruthenium(II) Complexes as Dual Catalytic Inhibitors of Topoisomerase I/II, *Angew. Chem., Int. Ed.*, 2020, **59**(38), 16631–16637.
- 75 W. Li, S. Li, G. Xu, X. Man, T. Yang, Z. Zhang, H. Liang and F. Yang, Developing a Ruthenium(III) Complex to Trigger Gasdermin E-Mediated Pyroptosis and an Immune Response Based on Decitabine and Liposomes: Targeting Inhibition of Gastric Tumor Growth and Metastasis, *J. Med. Chem.*, 2023, **66**(18), 13072–13085.
- 76 S. Li, H. Yuan, Y. Chen and Z. Guo, Metal complexes induced ferroptosis for anticancer therapy, *Fundam. Res.*, 2022, **3**(4), 525–528.
- 77 M. Zhou, J. C. Boulos, E. A. Omer, H. A. Rudbari, T. Schirmeister, N. Micale and T. Efferth, Two palladium(II) complexes derived from halogen-substituted Schiff bases and 2-picolylamine induce parthanatos-type cell death in sensitive and multi-drug resistant CCRF-CEM leukemia cells, *Eur. J. Pharmacol.*, 2023, **956**, 175980.
- 78 Z. Y. Lee, C. H. Leong, K. U. L. Lim, C. C. S. Wong, P. Pongtheerawan, S. A. Arikrishnan, K. L. Tan, J. S. Loh, M. L. Low, C. W. How, Y. S. Ong, Y. S. Tor and J. B. Foo, Induction of Apoptosis and Autophagy by Ternary Copper Complex Towards Breast Cancer Cells, *Anticancer Agents Med. Chem.*, 2022, **22**(6), 1159–1170.
- 79 G. D. Zhang, M. M. Wang, Y. Su, H. Fang, X. L. Xue, H. K. Liu and Z. Su, Mitochondria-targeted ruthenium complexes can be generated in vitro and in living cells to target triple-negative breast cancer cells by autophagy inhibition, *J. Inorg. Biochem.*, 2024, **256**, 112574.
- 80 Z. Xu, M. Xu, X. Wu, S. Guo, Z. Tian, D. Zhu, J. Yang, J. Fu, X. Li, G. Song, Z. Liu and X. Song, A Half-Sandwich Ruthenium(II) (N<sup>N</sup>) Complex: Inducing Immunogenic Melanoma Cell Death in Vitro and in Vivo, *ChemMedChem*, 2023, **18**(16), e202300131.
- 81 Z. Yang, M. Bian, L. Lv, X. Chang, Z. Wen, F. Li, Y. Lu and W. Liu, Tumor-Targeting NHC-Au(I) Complex Induces Immunogenic Cell Death in Hepatocellular Carcinoma, *J. Med. Chem.*, 2023, **66**(6), 3934–3952.
- 82 P. Kaur, A. Johnson, J. Northcote-Smith, C. Lu and K. Suntharalingam, Immunogenic Cell Death of Breast Cancer Stem Cells Induced by an Endoplasmic Reticulum-Targeting Copper(II) Complex, *Chem. Bio. Chem.*, 2020, **21**(24), 3618–3624.
- 83 S. Li, H. Yuan, Y. Chen and Z. Guo, Metal complexes induced ferroptosis for anticancer therapy, *Fundam. Res.*, 2023, **3**(4), 525–528.
- 84 X. Chen, P. B. Comish, D. Tang and R. Kang, Characteristics and biomarkers of ferroptosis, *Front. Cell Dev. Biol.*, 2021, **9**, 637162.
- 85 P. Wan, J. Yan and Z. Liu, Methodological advances in necroptosis research: from challenges to solutions, *J. Natl. Cancer Cent.*, 2022, **2**(4), 291–297.
- 86 C. Sanjai, S. S. Hakkimane, B. R. Guru and S. L. Gaonkar, A comprehensive review on anticancer evaluation techniques, *Bioorg. Chem.*, 2024, **142**, 106973.
- 87 S. Sen, M. Won, M. S. Levine, Y. Noh, A. C. Sedgwick, J. S. Kim, J. L. Sessler and J. F. Arambula, Metal-based anticancer agents as immunogenic cell death inducers: the past, present, and future, *Chem. Soc. Rev.*, 2022, **51**, 1212–1233.
- 88 G. L. Cohen, W. R. Bauer, J. K. Barton and S. J. Lippard, Binding of cis- and trans-Dichlorodiammineplatinum(II) to DNA: Evidence for Unwinding and Shortening of the Double Helix, *Science*, 1979, **203**, 1014–1016.
- 89 D. Wang and S. J. Lippard, Cellular processing of platinum anticancer drugs, *Nat. Rev. Drug Discovery*, 2005, **4**(4), 307–320.
- 90 R. C. Todd and S. J. Lippard, Inhibition of transcription by platinum antitumor compounds, *Metallomics*, 2009, **1**(4), 280–291.
- 91 G. Zhu, M. Myint, W. H. Ang, L. Song and S. J. Lippard, Monofunctional platinum-DNA adducts are strong inhibitors of transcription and substrates for nucleotide excision repair in live mammalian cells, *Cancer Res.*, 2012, **72**(3), 790–800.
- 92 A. Ashkenazi and V. M. Dixit, Death receptors: signaling and modulation, *Science*, 1998, **281**(5381), 1305–1308.
- 93 S. Elmore, Apoptosis: a review of programmed cell death, *Toxicol. Pathol.*, 2007, **35**(4), 495–516.
- 94 S.-W. Ryu, S.-J. Lee, M.-Y. Park, J.-i. Jun, Y.-K. Jung and E. Kim, Fas-associated Factor 1, FAF1, Is a Member of Fas Death-inducing Signaling Complex, *J. Biochem.*, 2003, **278**(26), 24003–24010.
- 95 C. Fernandes, A. Horn, B. F. Lopes, E. S. Bull, N. F. B. Azeredo, M. M. Kanashiro, F. V. Borges, A. J. Bortoluzzi, B. Szpoganicz, A. B. Pires, R. W. A. Franco, J. C. d. A. Almeida, L. L. F. Maciel, J. A. L. C. Resende and G. Schenk, Induction of apoptosis in leukemia cell lines by new copper(II) complexes containing naphthyl groups via interaction with death receptors, *J. Inorg. Biochem.*, 2015, **153**, 68–87.
- 96 X. Zhang, K. Selvaraju, A. A. Saei, P. D'Arcy, R. A. Zubarev, E. S. J. Arnér and S. Linder, Repurposing of auranofin: Thioredoxin reductase remains a primary target of the drug, *Biochimie*, 2019, **162**, 46–54.
- 97 H. Hwang-Bo, J. W. Jeong, M. H. Han, C. Park, S. H. Hong, G. Y. Kim, S. K. Moon, J. Cheong, W. J. Kim, Y. H. Yoo and Y. H. Choi, Auranofin, an inhibitor of thioredoxin reductase, induces apoptosis in hepatocellular carcinoma Hep3B cells by generation of reactive oxygen species, *Gen. Physiol. Biophys.*, 2017, **36**(2), 117–128.
- 98 G. Moreno-Alcántar, P. Picchetti and A. Casini, Gold Complexes in Anticancer Therapy: From New Design Principles to Particle-Based Delivery Systems, *Angew. Chem., Int. Ed.*, 2023, **62**, e202218000.
- 99 D. R. Green and G. Kroemer, The pathophysiology of mitochondrial cell death, *Science*, 2004, **305**(5684), 626–629.

- 100 A. Cossarizza and S. Salvioli, Flow cytometric analysis of mitochondrial membrane potential using JC-1, *Curr. Protoc. Cytom.*, 2001, DOI: [10.1002/0471142956.cy0914s13](https://doi.org/10.1002/0471142956.cy0914s13).
- 101 S. Riedl and G. Salvesen, The apoptosome: signalling platform of cell death, *Nat. Rev. Mol. Cell Biol.*, 2007, **8**, 405–413.
- 102 U. Jungwirth, C. R. Kowol, B. K. Keppler, C. G. Hartinger, W. Berger and P. Heffeter, Anticancer activity of metal complexes: involvement of redox processes, *Antioxid. Redox Signaling*, 2011, **15**(4), 1085–1127.
- 103 C. Gorrini, I. Harris and T. Mak, Modulation of oxidative stress as an anticancer strategy, *Nat. Rev. Drug Discovery*, 2013, **12**, 931–947.
- 104 L. Kubickova, L. Pour, L. Sedlarikova, R. Hajek and S. Sevcikova, Proteasome inhibitors - molecular basis and current perspectives in multiple myeloma, *J. Cell. Mol. Med.*, 2014, **8**(6), 947–961.
- 105 C. Hetz, K. Zhang and R. J. Kaufman, Mechanisms, regulation and functions of the unfolded protein response, *Nat. Rev. Mol. Cell Biol.*, 2020, **21**, 421–438.
- 106 M. Zaki, S. Hairatb and E. S. Aazama, Scope of organometallic compounds based on transition metal-arene systems as anticancer agents: starting from the classical paradigm to targeting multiple strategies, *RSC Adv.*, 2019, **9**, 3239–3278.
- 107 A. A. Al-Karmalawy, H. I. El-Subbagh, L. Logoyda, R. B. Lesyk and M. I. El-Gamal, Editorial: Recent advances in the research and development of kinase-inhibitory anticancer molecules, *Front. Chem.*, 2023, **11**, 1328424.
- 108 K. Kwan, O. Castro-Sandoval, C. Gaiddon and T. Storr, Inhibition of p53 protein aggregation as a cancer treatment strategy, *Curr. Opin. Chem. Biol.*, 2023, **72**, 102230.
- 109 S. Adhikari, P. Nath, A. Das, A. Datta, N. Baildya, A. K. Duttaroy and S. Pathak, A review on metal complexes and its anti-cancer activities: Recent updates from in vivo studies, *Biomed. Pharmacother.*, 2024, **171**, 116211.
- 110 K. Suntharalingam, O. Mendoza, A. A. Duarte, D. J. Mann and R. Vilar, A platinum complex that binds non-covalently to DNA and induces cell death via a different mechanism than cisplatin, *Metallomics*, 2013, **5**(5), 514–523.
- 111 K. Mitra, U. Basu, I. Khan, B. Maity, P. Kondaiah and A. R. Chakravarty, Remarkable anticancer activity of ferrocenyl terpyridine platinum(II) complexes in visible light with low dark toxicity, *Dalton Trans.*, 2014, **43**, 751–763.
- 112 K.-C. Tong, P.-K. Wan, C.-N. Lok and C.-M. Che, Dynamic supramolecular self-assembly of platinum(II) complexes perturbs an autophagy lysosomal system and triggers cancer cell death, *Chem. Sci.*, 2021, **12**, 15229–15238.
- 113 A. D. Aputen, M. G. Elias, J. Gilbert, J. A. Sakoff, C. P. Gordon, K. F. Scott and J. R. Aldrich-Wright, Platinum(IV) Prodrugs Incorporating an Indole-Based Derivative, 5-Benzyloxyindole-3-Acetic Acid in the Axial Position Exhibit Prominent Anticancer Activity, *Int. J. Mol. Sci.*, 2024, **25**(4), 2181.
- 114 M. G. Elias, S. Fatima, T. J. Mann, S. Karan, M. Mikhael, P. de Souza, C. P. Gordon, K. F. Scott and J. R. Aldrich-Wright, Anticancer Effect of Pt<sup>II</sup>PHENSS, Pt<sup>II</sup>5MESS, Pt<sup>II</sup>56MESS and Their Platinum(IV)-Dihydroxy Derivatives against Triple-Negative Breast Cancer and Cisplatin-Resistant Colorectal Cancer, *Cancers*, 2024, **16**, 2544.
- 115 L. Tabrizi, A. M. Jones, I. Romero-Canelon and A. Erxleben, Multiaction Pt(IV) Complexes: Cytotoxicity in Ovarian Cancer Cell Lines and Mechanistic Studies, *Inorg. Chem.*, 2024, **63**, 14958–14968.
- 116 J. N. Boodram, I. J. McGregor, P. M. Bruno, P. B. Cressey, M. T. Hemann and K. Suntharalingam, Breast Cancer Stem Cell Potent Copper(II)-Non-Steroidal Anti-Inflammatory Drug Complexes, *Angew. Chem., Int. Ed.*, 2016, **55**(8), 2845–2850.
- 117 B.-L. Fei, S. Tu, Z. Wei, P. Wang, C. Qiao and Z.-F. Chen, Optically pure chiral copper(II) complexes of rosin derivative as attractive anticancer agents with potential anti-metastatic and anti-angiogenic activities, *Eur. J. Med. Chem.*, 2019, **176**, 175–186.
- 118 C. Icsel, V. T. Yilmaz, Ş. Aydinlik and M. Aygun, New manganese(II), iron(II), cobalt(II), nickel(II) and copper(II) saccharinate complexes of 2,6-bis(2-benzimidazolyl)pyridine as potential anticancer agents, *Eur. J. Med. Chem.*, 2020, **202**, 112535.
- 119 S. S. Hindo, M. Frezza, D. Tomco, M. J. Heeg, L. Hryhoreczuk, B. R. McGarvey, Q. P. Dou and C. N. Verani, Metals in anticancer therapy: Copper(II) complexes as inhibitors of the 20S proteasome, *Eur. J. Med. Chem.*, 2009, **44**, 4353–4361.
- 120 B. L. Fei, C. N. Hui, Z. Wei, L. Y. Kong, J. Y. Long, C. Qiao and Z.-F. Chen, Copper(II) and iron(III) complexes of chiral dehydroabiatic acid derived from natural rosin: metal effect on structure and cytotoxicity, *Metallomics*, 2021, **13**(4), mfab014.
- 121 Y. Li, Q. Wu, G. Yu, L. Li, X. Zhao, X. Huang and W. Mei, Polypyridyl Ruthenium(II) complex-induced mitochondrial membrane potential dissipation activates DNA damage-mediated apoptosis to inhibit liver cancer, *Eur. J. Med. Chem.*, 2019, **164**, 282–291.
- 122 C. Chen, C. Xu, T. Li, S. Lu, F. Luo and H. Wang, Novel NHC-coordinated ruthenium(II) arene complexes achieve synergistic efficacy as safe and effective anticancer therapeutics, *Eur. J. Med. Chem.*, 2020, **203**, 112605.
- 123 J. Chen, J. Wang, Y. Deng, B. Li, C. Li, Y. Lin, D. Yang, H. Zhang, L. Chen and T. Wang, Novel cyclometalated Ru(II) complexes containing isoquinoline ligands: Synthesis, characterization, cellular uptake and *in vitro* cytotoxicity, *Eur. J. Med. Chem.*, 2020, **203**, 112562.
- 124 M. Allison, P. Caramés-Méndez, B. J. Hofmann, C. M. Pask, R. M. Phillips, R. M. Lord and P. C. McGowan, Cytotoxicity of Ruthenium(II) Arene Complexes Containing Functionalized Ferrocenyl  $\beta$ -Diketonate Ligands, *Organometallics*, 2023, **42**, 1869–1881.
- 125 R. Pettinari, C. Pettinari, F. Marchetti, B. W. Skelton, A. H. White, L. Bonfili, M. Cuccioloni, M. Mozzicafreddo,

- V. Cecarini, M. Angeletti, M. Nabissi and A. M. Eleuteri, Arene-ruthenium(II) acylpyrazolonato complexes: apoptosis-promoting effects on human cancer cells., *J. Med. Chem.*, 2014, **57**(11), 4532–4542.
- 126 D. Truong, M. P. Sullivan, K. K. H. Tong, T. R. Steel, A. Prause, J. H. Lovett, J. W. Andersen, S. M. F. Jamieson, H. H. Harris, I. Ott, C. M. Weekley, K. Hummitzsch, T. Söhnle, M. Hanif, N. Metzler-Nolte, D. C. Goldstone and C. G. Hartinger, Potent Inhibition of Thioredoxin Reductase by the Rh Derivatives of Anticancer M(arene/Cp\*)(NHC)Cl<sub>2</sub> Complexes, *Inorg. Chem.*, 2020, **59**(5), 3281–3289.
- 127 E. Atrián-Blasco, S. Gascón, M. J. Rodríguez-Yoldi, M. Laguna and E. Cerrada, Novel Gold(I) Thiolate Derivatives Synergistic with 5 Fluorouracil as Potential Selective Anticancer Agents in Colon Cancer, *Inorg. Chem.*, 2017, **56**, 8562–8579.
- 128 I. Mármol, M. Virumbrales-Muñoz, J. Quero, C. Sánchez-de-Diego, L. Fernández, I. Ochoa, E. Cerrada and M. J. Rodríguez-Yoldi, Alkynyl gold(I) complex triggers necroptosis via ROS generation in colorectal carcinoma cells, *J. Inorg. Biochem.*, 2017, **176**, 123–133.
- 129 J. Quero, J. C. Royo, B. Fodor, M. C. Gimeno, J. Osada, M. J. Rodríguez-Yoldi and E. Cerrada, Sulfonamide-Derived Dithiocarbamate Gold(I) Complexes Induce the Apoptosis of Colon Cancer Cells by the Activation of Caspase 3 and Redox Imbalance, *Biomedicines*, 2022, **10**, 1437.
- 130 A. Gutiérrez, L. Gracia-Fleta, I. Marzo, C. Cativiela, A. Laguna and M. C. Gimeno, Gold(I) thiolates containing amino acid moieties: Cytotoxicity and structure–activity relationship studies, *Dalton Trans.*, 2014, **43**, 17054–17066.
- 131 Y. Li, Z. Gu, C. Zhang, S. Li, L. Zhang, G. Zhou, S. Wang and J. Zhang, Synthesis, characterization and ROS-mediated antitumor effects of palladium(II) complexes of curcuminoids, *Eur. J. Med. Chem.*, 2018, **144**, 662–671.
- 132 K. Karami, N. Jamshidian, M. Zakariazadeh, A. A. Momtazi-Borojeni, E. Abdollahi, Z. Amirghofran, A. Shahpiri and A. K. Nasab, Experimental and theoretical studies of Palladium-hydrazide complexes' interaction with DNA and BSA, in vitro cytotoxicity activity and plasmid cleavage ability, *Comput. Biol. Chem.*, 2021, **91**, 107435.